Mitotic Spindle Integrity and Kinetochore Function Linked by the Duo1p/Dam1p Complex

Iain M. Cheeseman, Maria Enquist-Newman, Thomas Müller-Reichert, David G. Drubin, and Georjana Barnes

Department of Molecular and Cell Biology, University of California at Berkeley, Berkeley, California 94720

Abstract. Duo1p and Dam1p were previously identified as spindle proteins in the budding yeast, *Saccharomyces cerevisiae*. Here, analyses of a diverse collection of *duo1* and *dam1* alleles were used to develop a deeper understanding of the functions and interactions of Duo1p and Dam1p. Based on the similarity of mutant phenotypes, genetic interactions between *duo1* and *dam1* alleles, interdependent localization to the mitotic spindle, and Duo1p/Dam1p coimmunoprecipitation from yeast protein extracts, these analyses indicated that Duo1p and Dam1p perform a shared function in vivo as components of a protein complex. Duo1p and Dam1p are not required to assemble bipolar spindles, but they are required to maintain metaphase and anaphase spindle integrity. Immunofluorescence and electron microscopy of *duo1* and *dam1* mutant spindles revealed a diverse variety of spindle defects. Our results also indicate a second, previously unidentified, role for the Duo1p/Dam1p complex. *duo1* and *dam1* mutants show high rates of chromosome missegregation, premature anaphase events while arrested in metaphase, and genetic interactions with a subset of kinetochore components consistent with a role in kinetochore function. In addition, Duo1p and Dam1p localize to kinetochores in chromosome spreads, suggesting that this complex may serve as a link between the kinetochore and the mitotic spindle.

Key words: microtubule • spindle • mitosis • kinetochore • *Saccharomyces cerevisiae*

Introduction

To carry out chromosome segregation faithfully during mitosis, the mitotic spindle must undergo precise changes at appropriate cell cycle stages (for a review see Botstein et al., 1997). In budding yeast, the microtubule organizing center, or spindle pole body (SPB),[1] duplicates after passage through G_1. A bipolar spindle then assembles and establishes attachments to each pair of sister chromatids. At this stage, cohesion between sister chromatids prevents the spindle from elongating past a metaphase length of ~1–2 μm (Michaelis et al., 1997). At the onset of anaphase, chromatid cohesion is eliminated by action of the anaphase promoting complex (APC), a ubiquitin ligase that targets several proteins for degradation during mitosis (King et al., 1995). With the loss of cohesion, sister chromatid separation and spindle elongation can occur to segregate the chromosomes. Finally, after spindle elongation, the spindle breaks down as the cells exit mitosis.

The mitotic spindle is primarily composed of microtubules. However, several other proteins are required for spindle assembly, function, and regulation (for a review see Sobel, 1997; Winsor and Schiebel, 1997). In yeast, spindle proteins include the kinesin-related motors Cin8p, Kip1p, and Kar3p (Roof et al., 1992; Saunders and Hoyt, 1992; Saunders et al., 1997), which provide the forces and structure required to assemble a bipolar spindle and to facilitate spindle elongation. There are also nonmotor microtubule-associated proteins such as Stu1p (Pasqualone and Huffaker, 1994), Ase1p, and Bim1p that are associated with mitotic spindles. Ase1p plays a structural role by cross-linking microtubules in the spindle midzone (Pellman et al., 1995). Bim1p has an incompletely understood role in spindle function (Schwartz et al., 1997; Tirnauer et al., 1999), as well as a role in cytoplasmic microtubule–mediated spindle migration and orientation (Korinek et al., 2000; Lee et al., 2000).

In addition to the structural and mechanical components required to form a functional spindle, other factors are needed to attach the chromosomes to spindle microtubules. This attachment occurs at kinetochores, multiprotein complexes associated with centromeric DNA. Although the organization of the DNA-binding components of the yeast kinetochore has been characterized (Sorger et al., 1994; Espelin et

Address correspondence to Georjana Barnes, 401 Barker Hall #3202, University of California at Berkeley, Berkeley, CA 94720-3202. Tel.: (510) 642-5962. Fax: (510) 643-0062. E-mail: gbarnes@socrates.berkeley.edu

[1]*Abbreviations used in this paper:* APC, anaphase promoting complex; GFP, green fluorescent protein; HU, hydroxyurea; SPB, spindle pole body; YPD, yeast extract/peptone plus dextrose.

al., 1997; Meluh and Koshland, 1997), complete elucidation of kinetochore activities requires the identification of all of the proteins involved. In addition, the mechanism by which the kinetochore attaches to spindle microtubules, and how this attachment is regulated, remain to be determined.

Changes in the mitotic spindle, particularly the transition to anaphase spindle elongation, are under tight cell cycle control. In addition to the regulation by the APC and the cyclin-dependent kinase, Cdc28p, spindle function is also monitored by the spindle assembly checkpoint. This checkpoint regulation is mediated by at least seven proteins: Mad1p, Mad2p, Mad3p, Bub1p, Bub2p, Bub3p, and Mps1p (Hoyt et al., 1991; Li and Murray, 1991; Weiss and Winey, 1996). In response to spindle damage or an unattached kinetochore, the spindle assembly checkpoint directly inhibits the Cdc20p-bound form of the APC resulting in a metaphase arrest (Hwang et al., 1998). In yeast, this arrest results in a large-budded cell with a short mitotic spindle and undivided DNA.

Previous work suggested that the *S. cerevisiae* proteins Duo1p and Dam1p are required for spindle function (Hofmann et al., 1998; Jones et al., 1999). Two-hybrid analysis and in vitro binding studies indicated that these proteins interact with each other physically. Both Duo1p and Dam1p localize along the length of the mitotic spindle, and Dam1p binds directly to microtubules in vitro. Moreover, temperature-sensitive mutants of both genes show spindle defects. Here, we characterize a collection of novel temperature-sensitive alleles of *duo1* and *dam1*. Our analyses show that Duo1p and Dam1p form a conserved protein complex in vivo that is required for diverse aspects of spindle integrity and for kinetochore function.

Materials and Methods

Strains and Growth Conditions

Yeast strains used in this study are listed in Table I. *mad2*Δ (pRC4) and *mad3*Δ (pKH502) deletions (Chen et al., 1999; Hardwick et al., 2000), Pds1-myc18 fusion (Ciosk et al., 1998), LacI-GFP/LacO System (pSB116 and pAFS59) (Straight et al., 1996; Biggins et al., 1999), and Ndc10-GFP fusion (Zeng et al., 1999) were generated in our strain background. Yeast were grown on either yeast extract/peptone or synthetic medium supplemented with the appropriate nutrients and 2% glucose, or 2% galactose and 2% raffinose, using standard procedures (Rose et al., 1990). All growth experiments were conducted in yeast extract/peptone plus dextrose (YPD). Benomyl sensitivity was tested on 10, 15, and 20 μg/ml benomyl in YPD. Wild-type strains grew at all concentrations, though more slowly at the higher concentrations. Alpha factor arrest was conducted in fresh medium containing 15–20 μg/ml alpha factor (Bar^+ strains), and hydroxyurea (HU) arrest was conducted by adding 0.1–0.2 M HU directly to the medium. Geneticin (G418; GIBCO BRL) was used at an effective concentration of 0.4 mg/ml. Temperature shift experiments were conducted by diluting an overnight culture, growing these cells to log phase for 2 h at 25°C, and then shifting the cells to 37°C. For the cell morphology experiments, cells were fixed with 4% formaldehyde and sonicated briefly before counting. A cell was scored as large-budded if the daughter cell was at least half the size of the mother, and 300 cells were counted for each time point. For the LacI-GFP experiments, cells were grown in YPD with 250 μM $CuSO_4$ to induce expression of the LacI-GFP fusion and an additional 0.02% adenine to reduce background fluorescence. Viability experiments were conducted by plating dilutions equivalent to 10^{-2} and 10^{-3} μl of cells at the permissive temperature and comparing colonies formed to total cells plated. A fixed sample of cells corresponding to 0.02 μl was counted for each sample using a hemacytometer (Fisher Scientific).

Sequence Analysis

Homologues of Duo1p and Dam1p were identified using a basic local alignment search tool (BLAST) of the *Candida albicans* (http://www-sequence.stanford.edu/group/candida), *Aspergillus nidulans* (http://www.genome.ou.edu/fungal.html), and *Schizosaccharomyces pombe* (http://www.sanger.ac.uk/Projects/S_pombe), using the *S. cerevisiae* or *C. albicans* Duo1p or Dam1p amino acid sequence. Sequences were aligned using ClustalW from European Bioinformatics Institute (http://www2.ebi.ac.uk/clustalw/) and formatted using the Seqvu 1.0 software (Garvan Institute of Medical Research). Coiled coil regions were predicted using the COILS program (http://www.ch.embnet.org/software/COILS_form.html), and the leucine zipper motif was identified using PROSITE (http://www.expasy.ch/prosite/). All programs were used with standard settings.

Immunofluorescence Microscopy

Chromosome spreads were prepared as described (Loidl et al., 1998). Lipsol was obtained from Lip Ltd. To depolymerize microtubules for these chromosome spreads, 20 μg/ml nocodazole was added to the growing cells for 1 h. In addition, 20 μg/ml nocodazole was included in the sorbitol buffer during zymolyase treatment. Indirect immunofluorescence microscopy on intact yeast cells was performed as described (Ayscough and Drubin, 1998). The YOL134 antitubulin antibody (Accurate Chemical and Scientific Corporation) was used at a dilution of 1:200, rabbit anti-GFP antibody (a generous gift from Pam Silver, Harvard Medical School, Boston, MA) at 1:4,000, mouse anti-GFP antibody (Roche), rabbit anti-Tub4p antibody (a generous gift from Tim Stearns, Stanford University, Stanford) at 1:1,000, affinity-purified rabbit anti-Duo1p antibody (Hofmann et al., 1998) at 1:2,000, and affinity-purified guinea pig anti-Dam1p antibody (preparation described below) at 1:1,000. Fluorescein- or rhodamine-conjugated anti-IgG heavy chain secondary antibodies (Cappel/Organon Technika Inc. or Jackson ImmunoResearch Laboratories) were used at 1:500, and Cy3-conjugated goat anti–rabbit secondary antibody (Sigma-Aldrich) at 1:2,000. Light microscopy was performed using an Axiovert microscope equipped with a 100×/1.3 Plan-Neoflar oil immersion objective (ZEISS) and a Sensys charge-coupled device camera (Photometrics) controlled by Phase-3 software (Phase-3 Imaging Systems), or a Nikon TE300 microscope equipped with a 100×/1.4 Plan-Apo objective and a Orca-100 cooled charge-coupled device camera (Hamamatsu) controlled by Phase-3 software.

Electron Microscopy

Yeast cells were cryoimmobilized using an HPM 010 high pressure freezer (BAL-TEC). Samples were processed for freeze substitution as described previously (Winey et al., 1995). In brief, samples were freeze substituted at −90°C for 3 d in acetone containing either 0.2% glutaraldehyde and 0.1% uranyl acetate or 2% osmium tetroxide and 0.1% uranyl acetate. The temperature of the samples was raised progressively to room temperature over 48 h in an automatic freeze substitution machine (Leica). Samples were embedded in LR white epoxy or in epon/araldite. Thin sections (50 nm) were cut using a Ventana-RMC MT-X and a Reichert-Jung ULTRACUT E microtome. Sections were collected on Formvar-coated copper grids and poststained with 2% uranyl acetate in 70% methanol for 4 min followed by aqueous Reynolds' lead citrate for 2 min. Samples were imaged using either a JEOL 100 CX or a Philips TECNAI 12 transmission electron microscope operated at 80 or 100 kV, respectively.

Generation of Temperature-sensitive duo1 and dam1 Mutants

The *DAM1* open reading frame was subcloned into the BamHI and XbaI sites of pRS315 or pRS316 (Sikorski and Hieter, 1989) to generate pDD883 and pDD882, respectively, using primers oIC16 (CGC GCG GAT CCA CGA GCA CTG CCT AAA CGG) and oIC17 (CGC GCT CTA GAC CGT TGT CCA GTT TCT TGT C). *dam1* mutants were generated by random mutagenesis using two separate methods. *dam1-24* (subsequent sequencing revealed that this allele contained the same mutation as *dam1-1*; our data and Jones, M., and M. Winey, personal communication) and *dam1-19* were generated by mutagenesis of pDD883 (*DAM1*, *CEN*, *LEU2*) in vitro with hydroxylamine as described previously (Hofmann et al., 1998). *dam1-5*, *dam1-9*, *dam1-10*, and *dam1-11* were generated by PCR amplification of the *DAM1* open reading frame with Taq DNA polymerase and then by gap repair in vivo with pDD883 cut with Eco47III and NheI to remove the majority of the *DAM1* open reading frame. Mutagenized plasmids were transformed into haploid *dam1* deletion strain carrying pDD882 (*DAM1*, *CEN*, *URA3*) and were replica plated to 5-fluoroorotic acid to select against the wild-type plasmid. A total of 5,000 colonies were screened for the hydroxlyamine mutants, and 4,000 colonies were screened for the PCR-based mutants. Two isolates of *dam1-5* and seven isolates of

Table I. Yeast Strains Used in this Study

Name	Genotype	Source
DDY1900	*MATa/MATα, his3Δ200/his3Δ200, leu2-3,112/leu2-3,112, ura3-52/ura3-52, ade2-1/+, lys2-801/+, dam1Δ::HIS3/DAM1*	This study
DDY902	*MATa, his3Δ200, leu2-3,112, ura3-52, ade2-1*	Drubin lab*
DDY904	*MATα, his3Δ200, leu2-3,112, ura3-52, lys2-801*	Drubin lab*
DDY1901	*MATa, his3Δ200, leu2-3,112, ura3-52, ade2-1, duo1-1::LEU2*	Drubin lab*
DDY1524	*MATα, his3Δ200, leu2-3,112, ura3-52, lys2-801, duo1-1::LEU2*	Drubin lab*
DDY1902	*MATa, his3Δ200, leu2-3,112, ura3-52, ade2-1, duo1-2::LEU2*	Drubin lab*
DDY1525	*MATα, his3Δ200, leu2-3,112, ura3-52, lys2-801, duo1-2::LEU2*	Drubin lab*
DDY1903	*MATa, his3Δ200, leu2-3,112, ura3-52, ade2-1, dam1-5::KanMX*	This study
DDY1904	*MATα, his3Δ200, leu2-3,112, ura3-52, lys2-801, dam1-5::KanMX*	This study
DDY1905	*MATa, his3Δ200, leu2-3,112, ura3-52, ade2-1, dam1-9::KanMX*	This study
DDY1906	*MATα, his3Δ200, leu2-3,112, ura3-52, lys2-801, dam1-9::KanMX*	This study
DDY1907	*MATa, his3Δ200, leu2-3,112, ura3-52, ade2-1, dam1-10::KanMX*	This study
DDY1908	*MATα, his3Δ200, leu2-3,112, ura3-52, lys2-801, dam1-10::KanMX*	This study
DDY1909	*MATa, his3Δ200, leu2-3,112, ura3-52, ade2-1, dam1-11::KanMX*	This study
DDY1910	*MATα, his3Δ200, leu2-3,112, ura3-52, lys2-801, dam1-11::KanMX*	This study
DDY1911	*MATa, his3Δ200, leu2-3,112, ura3-52, ade2-1, dam1-19::KanMX*	This study
DDY1912	*MATα, his3Δ200, leu2-3,112, ura3-52, lys2-801, dam1-19::KanMX*	This study
DDY1913	*MATa, his3Δ200, leu2-3,112, ura3-52, ade2-1, dam1-1::KanMX*	This study
DDY1914	*MATα, his3Δ200, leu2-3,112, ura3-52, lys2-801, dam1-1::KanMX*	This study
DDY1915	*MATa, his3Δ200, leu2-3,112, ade2-1, duo1Δ::HIS3, ura3-52::duo1^{td}::URA3*	This study
DDY1916	*MATα, his3Δ200, leu2-3,112, lys2-801, duo1Δ::HIS3, ura3-52::duo1^{td}::URA3*	This study
DDY1788	*MATa, his3Δ200, leu2-3,112, ura3-52, ade2-1, mad2Δ::URA3*	This study
DDY1789	*MATa, his3Δ200, leu2-3,112, ura3-52, ade2-1, mad3Δ::URA3*	This study
DDY1526	*MATα, his3Δ200, leu2-3,112, ura3-52, ade2-1, lys2-801, duo1-2::LEU2, mad2Δ::URA3*	Drubin lab*
DDY1917	*MATa, his3Δ200, leu2-3,112, ura3-52, dam1-5::KanMX, mad2Δ::URA3*	This study
DDY1918	*MATa, his3Δ200, leu2-3,112, ura3-52, lys2-801, dam1-9::KanMX, mad2Δ::URA3*	This study
DDY1919	*MATa, his3Δ200, leu2-3,112, ura3-52, lys2-801, dam1-11::KanMX, mad3Δ::URA3*	This study
DDY1920	*MATa, his3Δ200, leu2-3,112, ura3-52, ade2-1, dam1-1::KanMX, mad3Δ::URA3*	This study
DDY1921	*MATa, his7, ura1, cdc15-1*	Andrew Murray
DDY1922	*MATa, ade2-1, his, ura, duo1-2::LEU2, mad2Δ::URA3, cdc15-1*	This study
DDY1923	*MATa, leu2-3,112, lys2-801 his, ura, dam1-9::KanMX, mad2Δ::URA3, cdc15-1*	This study
DDY1924	*MATa, leu2-3,112, his, ura, dam1-11::KanMX, mad3Δ::URA3, cdc15-1*	This study
DDY1925	*MATa, his3Δ200, ura3-52, ade2-1, HIS3::pCu-LacI-GFP, leu2-3,112::lacO::LEU2*	This study
DDY1926	*MATα, his3Δ200, ura3-52, ade2-1, HIS3::pCu-LacI-GFP, leu2-3,112::lacO::LEU2, dam1-11::KanMX*	This study
DDY1927	*MATa, his3Δ200, ura3-52, ade2-1, lys2-801, HIS3::pCu-LacI-GFP, leu2-3,112::lacO::LEU2, dam1-1::KanMX*	This study
DDY1928	*MATa, his3Δ200, ura3-52, ade2-1, HIS3::pCu-LacI-GFP, leu2-3,112::lacO::LEU2, duo1-2::LEU2, mad2Δ::URA3*	This study
DDY1929	*MATa, his3Δ200, ura3-52, ade2-1, leu2-3,112::PDS1-myc18::LEU2*	This study
DDY1930	*MATa, his3Δ200, ura3-52, lys2-801, leu2-3,112::PDS1-myc18::LEU2, dam1-9::KanMX*	This study
DDY1931	*MATa, his3Δ200, ura3-52, ade2-1, leu2-3,112::PDS1-myc18::LEU2, dam1-11::KanMX*	This study
DDY1581	*MATa, his3Δ200, his7, leu2-3,112, ura1, ade2-1, trp1-1, cdc16-1*	Andrew Murray
DDY1933	*MATa, his3Δ200, leu2-3,112, ura3-52, ade2-1, lys2-801, cdc16-1, dam1-9::KanMX*	This study
DDY1934	*MATa, his3Δ200, leu2-3,112, ura3-52, lys2-801, cdc26Δ::URA3, dam1-10::KanMX*	This study
DDY1935	*MATa, his3Δ200, leu2-3,112, ura3-52, lys2-801, cdc16-1, dam1-11::KanMX*	This study
DDY1936	*MATa, his3Δ200, leu2-3,112, ura3-52, trp1-1, cdc16-1, dam1-1::KanMX*	This study
DDY1937	*MATa, his3Δ200, ura3-52, leu2-3,112, cdc20Δ::LEU2, Gal-CDC20::TRP1*	Kim Naysmyth; This study
DDY1938	*MATa, his3Δ200, ura3-52, leu2-3,112, lys2-801, cdc20Δ::LEU2, Gal-CDC20::TRP1, dam1-11::KanMX*	This study
DDY1939	*MATα, his3Δ200, leu2-3,112, ura3-52, lys2-801, NDC10-GFP::HIS3*	This study
DDY1484	*MATα, lys2-801, ade2-101, his3Δ200, leu2-Δ1, ura3-52, TUB1::LYS2, bim1Δ::URA3*	David Botstein
DDY1514	*MATa, his3Δ200, leu2-3,112, ura3-52, lys2-801, trp1Δ1, mps1-1*	Mark Winey
DDY1529	*MATa, his3Δ200, leu2-3,112, ura3-52, stu1-5*	Tim Huffaker
DDY1806	*MATa, his3Δ200, leu2-3,112, ura3-52, ade2-101, cin8Δ::URA3*	M. Andy Hoyt
DDY1547	*MATa, leu2-3,112, ura3-52, ade2, ade3, ase1Δ1::URA3*	David Pellman
DDY1546	*MATα, ade2, ade3, leu2-3,112, ura3-52, trp1, bik1-1::TRP1*	David Pellman
DDY1504	*MATa, his3Δ200, leu2-3,112, ura3-52, lys2-801, bub1Δ::HIS3*	M. Andy Hoyt
DDY1505	*MATa, his3Δ200, leu2-3,112, ura3-52, ade2-101, lys2-801, bub3Δ::LEU2*	M. Andy Hoyt
DDY2088	*MATα, his3Δ200, leu2-3,112, ura3-52, lys2-801, trp1-1, bir1-Δ11::LEU2*	Clarence Chan
DDY1943	*MATa, his3Δ200, leu2Δ1, ura3-52, ade2-101, lys2-801, trp1Δ1, ctf19Δ::HIS3*	Phil Hieter

*All Drubin lab strains are derived from strain S288C.

dam1-11 were obtained from both PCR and hydroxylamine methods based on sequencing of the alleles.

Sequencing revealed that the *DAM1* sequence in our lab strain background (S288C) differed from the *Saccharomyces* Genome Database sequence by a frameshift 874 bp into the open reading frame. A similar sequence has also been observed in strains from the W303 background (Jones, M., and M. Winey, personal communication). This modified sequence (sequence data are available from GenBank/EMBL/DDBJ under accession no. AF280542) is shown in Fig. 1 A. Sequencing also revealed that *dam1-5* differs from *dam1-11* by a single additional point mutation. Since these two alleles have a similar growth range and spindle phenotype, they were considered similar for the purposes of this paper.

The *dam1* alleles were subsequently integrated into the genome. A NotI site was inserted ~150 bp downstream of the *DAM1* stop codon using the Transformer™ Site-Directed Mutagenesis Kit (CLONTECH Laboratories, Inc.) with the mutagenesis oligo oIC18 (CAG CAG TGC ATG GGC AGC GGC CGC ATT ACA ACG AAA C). The G418 resistance gene (KanMX) from pUG6 was cloned into the NotI site in the same orientation as the *DAM1* gene. *dam1* mutants were then swapped into this vector using the NheI and SacII sites and were

subsequently linearized for integration using SmaI and SacII. These fragments were then transformed into DDY1900, and G418$^+$His$^-$ diploids were selected. These diploids were then sporulated, and haploid integrants were recovered.

The degron-tagged allele of *duo1* (*duo1^{td}*) was generated by cloning *DUO1* into the HindIII sites of pPW66R (Dohmen et al., 1994). The *DUO1* open reading frame was amplified using the primers oIC31 (GCG CGA AGC TTC CGG GGG GAT GAG TGA GCA AAG CCA ATT AGA TG) and oIC32 (GCG CGA AGC TTA TCC TAG ATA CAT TCC CG). The resulting plasmid was then cut with NcoI and integrated into the *URA3* locus of a heterozygous *duo1* deletion strain. This strain was sporulated, and *duo1^{td}*::*URA3 duo1*Δ haploids were recovered.

Protein and Immunological Techniques

For protein immunoprecipitation from yeast extracts, 50 ml of yeast culture were grown to OD_{600} 1.2 in YPD, washed with sorbitol buffer (1.3 M sorbitol, 0.1 M potassium phosphate, pH 7.5), and incubated for 30 min with lyticase (Rothblatt and Schekman, 1989). Cells were pelleted gently and resuspended in lysis buffer (50 mM Tris-HCl, pH 8.0, 150 mM NaCl, 1% NP-40) with protease inhibitors and 1 mM PMSF. The resuspended cells were then sonicated three times for 15 s and pelleted at maximum speed in a microfuge. Approximately 6 μl of anti-Duo1p or anti-Dam1p antibody (see below) precoupled to 7 μl of Protein A Affi-gel beads (Bio-Rad Laboratories) was added to extract from 20 OD_{600} U of yeast. Samples were incubated overnight at 4°C, washed three times with lysis buffer, and sample buffer was added.

Yeast whole cell lysates were prepared as described (Belmont and Drubin, 1998). A total 0.17 OD_{600} U were loaded per lane of a 12% polyacrylamide gel prepared for SDS-PAGE (Laemmli, 1970) and were electrotransferred to BA83 Protran membrane (Schleicher & Schuell). Anti-Duo1p antibody was used at a dilution of 1:2,000, anti-Dam1p antibody at 1:1,000, B206 anti-tubulin antibody at 1:20,000 (a gift from Frank Solomon, University of California at Santa Cruz, Santa Cruz, CA), 9E10 anti-myc antibody (Santa Cruz Biotechnology, Inc.) at 1:2,000, anti-Clb2 antibody (a generous gift of Doug Kellogg, Massachusetts Institute of Technology, Cambridge, MA) at 1:2,000 with at least one with 0.5 M NaCl wash of the blot, and anti-GFP antibody at 1:10,000. HRP-conjugated secondary antibodies against rabbit, mouse (Amersham Life Sciences), and guinea pig (Alpha Diagnostic, Inc.) were used at 1:10,000.

Generation of Anti-Dam1p Antibody

The *DAM1* coding sequence was amplified from genomic DNA using the primers oCH52 (GCG GGA TCC ATG AGC GAA GAT AAA GCT AAA TTA GGG) and oIC24 (GCG CGC CAT GGA ACT CAC GCA TGC TAG CG), and the product was cloned into pRSETa (Invitrogen) in frame with a six-histidine tag to create pDD884. The construct was transformed into BL21 (DE3) cells, and expression of the fusion protein was induced by addition of 0.4 mM IPTG for 3.5 h at 37°C. Cells were lysed by sonication and spun for 15 min at 25,000 *g*; the pellet was resolubilized with 4 M urea. The denatured fusion protein was purified using a QIAGEN nickel-nitrilotriacetic acid column according to the manufacturer's guidelines and then dialyzed into 1 M urea in PBS with a total of 0.5 M NaCl and 5% glycerol.

Antibodies were generated by injecting guinea pigs with the purified protein (100 μg/injection, five injections at 3-wk intervals), using RIBI adjuvant (RIBI Immunochemical Research, Inc.). An affinity matrix was created by immobilizing the fusion protein on Affi-gel 10 resin (BioRad Laboratories) using the procedure described in the product manual. Clarified serum was circulated over the column overnight and washed first with buffer B (120 mM NaCl, 50 mM Tris-HCl, pH 8, 0.5% NP-40), next with 1 M LiCl, 50 mM Tris-HCl, pH 8, 0.5% NP-40, once more with buffer B, and finally with PBS. Specific antibodies were eluted with 50 mM glycine and 150 mM NaCl, pH 2.5. Peak fractions were dialyzed into PBS plus 35% glycerol and stored at −20°C.

Results

Mutagenesis of DUO1 and DAM1

Previous analyses of *DUO1* and *DAM1* were limited to only a few alleles: *dam1-1* (Jones et al., 1999), *duo1-1*, and *duo1-2* (Hofmann et al., 1998). *dam1-1* arrests with discontinuous spindles (Jones et al., 1999), a phenotype that is distinct from that described for alleles of *duo1*, which arrest with short spindles (Hofmann et al., 1998). Here, we used random mutagenesis of *DAM1* to generate six temperature-sensitive alleles (see Materials and Methods): *dam1-5*, *dam1-9*, *dam1-10*, *dam1-11*, *dam1-19*, and *dam1-24*. *dam1-24* was isolated by random mutagenesis, and we later found it to contain the same mutation as *dam1-1* (our data and Jones, M., and M. Winey, personal communication). Therefore, throughout the rest of this paper we will refer to *dam1-24* as *dam1-1*. To determine the null phenotype of *duo1*, we also generated a DHFR^{ts}-Duo1p fusion protein (referred to as *duo1^{td}*, for temperature degron [Dohmen et al., 1994]). This fusion protein is targeted for proteolysis at the restrictive temperature (not shown). Initial characterization of these novel *dam1* and *duo1* alleles showed a broad range of growth phenotypes, including a range of restrictive temperatures and sensitivities to the microtubule depolymerizing drug benomyl (Table II). Although we describe analyses of all these alleles here, we chose to focus primarily on *duo1-2*, *dam1-1*, *dam1-9*, and *dam1-11*, which all behave well at the permissive temperature and show a range of phenotypes at nonpermissive temperatures.

To identify the mutations present in each *dam1* allele, the mutants were sequenced. The complete results are summarized in Table II. To provide a better context for interpreting the mutations in the *dam1* and *duo1* alleles, we conducted BLAST searches for homologues of Dam1p and Duo1p in other organisms. Although we were not able to identify definitive metazoan homologues, homologues

Table II. Analysis of duo1 and dam1 Mutant Alleles

Allele	Class	Benomyl^S	Growth range				Mutations
			25°	30°	34°	37°	
duo1-2	1	No	Viable	Viable	Viable	Dead	A117T, M124I
duo1^{td}	2		Viable	Viable	Dead	Dead	"Degron tag"
dam1-1	2	Yes	Viable	Viable	Dead	Dead	C111Y
dam1-5	2	No	Viable	Medium growth defect	Dead	Dead	T58I, L98P, N139S, T332A
dam1-9	1	No	Viable	Viable	Medium growth defect	Dead	S97F, N139S, K170E, S328 P, T332A
dam1-10	3	Yes	Mild growth defect	Dead	Dead	Dead	L102S, C111R, N139S, T249I, N302D, T332A,I336Stop
dam1-11	2	No	Viable	Medium growth defect	Dead	Dead	L98P, N139S, T332A
dam1-19	4	No	Mild growth defect	Mild growth defect	Medium growth defect	Severe growth defect	Q205STOP

Class corresponds to the phenotype observed by immunofluorescence: 1, Short spindle arrest; 2, abnormal spindles; 3, hyperelongated spindles; and 4, collapsed spindles. *dam1-1* data are from Jones et al., 1999.

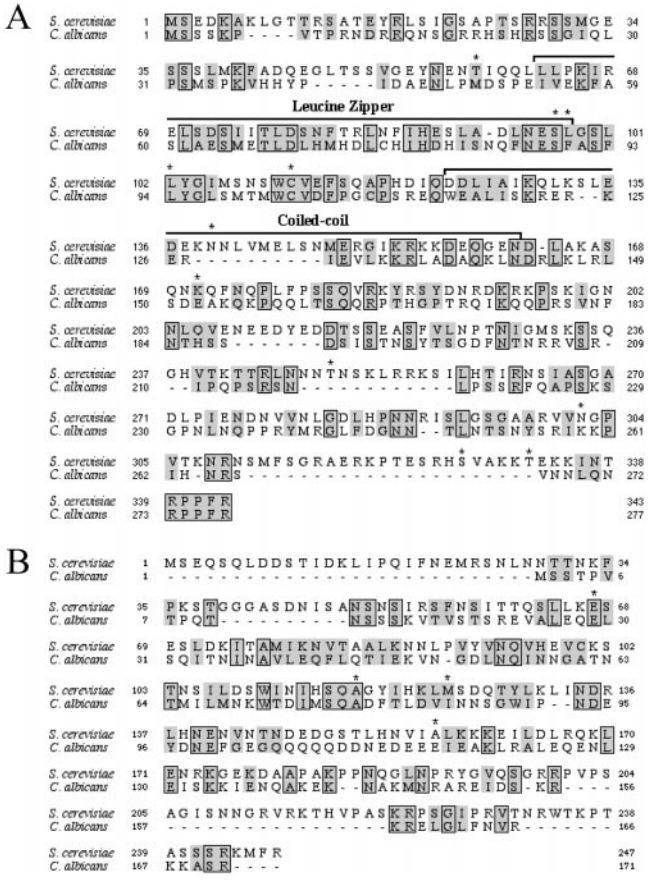

Figure 1. Dam1p and Duo1p mutations and *C. albicans* homologues. Identical residues are boxed and conserved residues are highlighted. Residues that are mutated in *duo1* or *dam1* mutants are indicated with an asterisk, with the exception of mutations to a stop codon (see Table II for a complete list of mutations in each allele). (A) Dam1p *C. albicans* homologue (orf5.6651). Both the leucine zipper region (residues 63–98) and the putative coiled coil region (residues 123–161) of Dam1p are conserved. These two proteins are 25% identical (70/277) and 53% conserved (147/277). *S. cerevisiae* Dam1p sequence data are available from GenBank/EMBL/DDBJ under accession no. AF280542. (B) Duo1p *C. albicans* homologue (orf5.4244). These two proteins are 21% identical (36/171) and 49% conserved (84/171).

were identified in several fungal species. The closest homologues for Dam1p (Fig. 1 A) and Duo1p (Fig. 1 B) were found in *Candida albicans*, although a Duo1p homologue was also identified in *Schizosaccharomyces pombe* (SPBC32F12.08c), and homologues for both proteins were found in *Aspergillus nidulans* (incomplete cDNA sequences n2d02a1.r1 for Duo1p, and r5a07a1.r1 for Dam1p). The predicted leucine zipper motif and coiled coil regions of Dam1p are conserved in *C. albicans* (Fig. 1 A). Many of the mutations in the *dam1* and *duo1* alleles were in residues that were conserved with the *C. albicans* homologues (Figs. 1, A and B).

To understand the functional relationship between Duo1p and Dam1p, and their relationship to other mitotic spindle proteins, we performed crosses between the alleles of *duo1* and *dam1*, and crosses between these alleles and other mutants that affect spindle function. Although our isolate of *dam1-1* has the same mutation as the previously published allele (Jones et al., 1999), we found some differences in its genetic interactions (see Table III). No intragenic complementation was observed for the collection of *dam1* alleles, suggesting that these alleles are defective in similar or overlapping functions. However, all six *dam1* alleles showed a strong genetic interaction with both *duo1-1* and *duo1-2* (Table III). To gain new insights into the spindle functions of Duo1p and Dam1p, we crossed *duo1* and *dam1* alleles to mutants with spindle defects (see Table III). *dam1-1* showed genetic interactions with *cin8*Δ and *stu1-5* consistent with previous reports for this allele (Jones et al., 1999). However, the other *duo1* and *dam1* mutants showed very weak, if any, interactions with these mutants. An additional allele-specific interaction was observed with the microtubule-associated protein, *bim1*Δ. Crosses were also made to *ase1*Δ and *bik1*Δ, but they did not show genetic interactions with *duo1-2*, *dam1-1*, *dam1-9*, or *dam1-11*. In addition, *duo1-2* was crossed to *kip3*Δ, *kar9*Δ, *dyn1*-Δ3, *stu2-10*, and *kip1*Δ, but no genetic interactions were observed. Some mutants with mitotic defects show genetic interactions with spindle assembly checkpoint components (Hardwick et al., 1999). In fact, we observed allele-specific genetic interactions with *mps1-1*, *mad2*Δ, *bub1*Δ, and *bub3*Δ (see Table III), but not with *mad3*Δ or *bub2*Δ. Finally, crosses were made to mutants defective in kinetochore function. No genetic interactions were observed with mutants of centromere DNA binding components *ndc10-1*,

Table III. Genetic Interactions

Allele	*duo1-2*	*duo1-1*	*cin8*Δ	*stu1-5*	*bim1*Δ	*mps1-1*	*mad2*Δ	*mad3*Δ	*bub1*Δ	*bub3*Δ	*bir1*Δ	*ctf19*Δ
duo1-2	-	-	Viable	Viable	Viable	Viable	∼Sick	Viable	Viable	Viable	Viable	
dam1-1	Lethal	Lethal	Lethal	Sick	Lethal	Lethal	Lethal	Viable	Lethal	Lethal	Lethal	Lethal
*dam1-1**	Lethal	Sick	Lethal	Sick		Lethal	Viable	Viable				
dam1-5	Lethal	Lethal	Viable	Viable		Viable	∼Sick					
dam1-9	Lethal	Sick	∼Sick	Viable	Viable	Viable	Viable		Viable	Viable	Viable	
dam1-10	Lethal					Lethal						
dam1-11	Lethal	Lethal	Viable	Viable	Viable	Viable	Sick	Viable	Lethal	Lethal	Viable	Viable
dam1-19	Lethal	Lethal	Viable	Viable			Viable					

For these genetic interactions, lethal is defined as the inability to recover viable double mutants at 25°C. Sick indicates a dramatic reduction in permissive temperature range for a double mutant compared with the individual single mutants. ∼Sick indicates a slight reduction in the permissive temperature range for the double mutant compared with the individual single mutants.

*Data are from Jones et al., 1999.

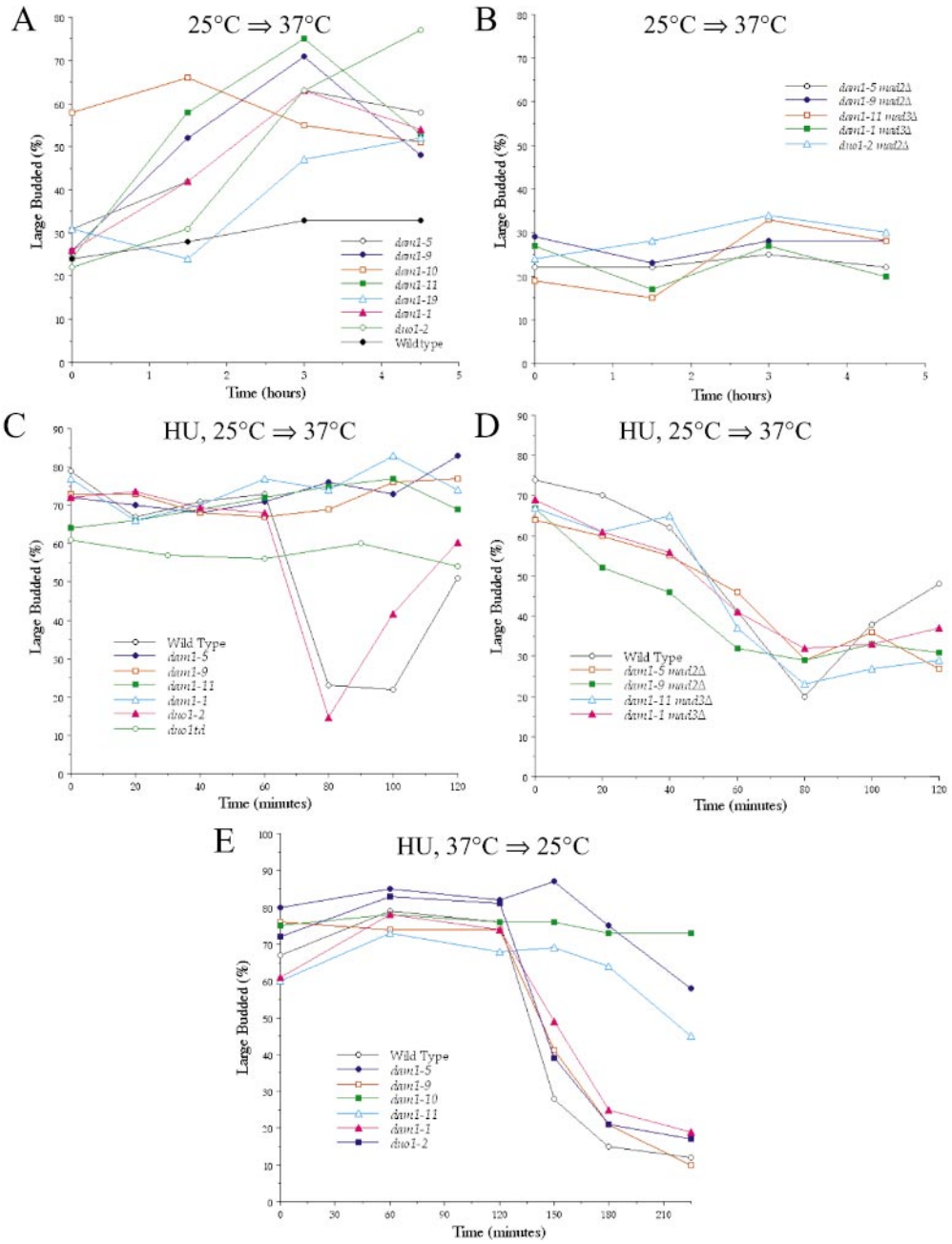

Figure 2. duo1 and *dam1* mutants arrest as large-budded cells in a spindle assembly checkpoint–dependent manner. (A and B) Cells were grown to log phase at 25°C and shifted to 37°C at $t = 0$. (C and D) Cells were grown to log phase and arrested with 0.2 M HU for ~4.5 h at 25°C. They were then released into fresh prewarmed medium lacking HU at 37°C ($t = 0$). (E) Cells were synchronized with alpha factor at 25°C and released into fresh prewarmed medium lacking alpha factor, but containing 0.2 M HU at 37°C. After 4 h, cells were released into fresh medium at 25°C ($t = 0$) with alpha factor to prevent reinitiation of the cell cycle.

ctf13-30, *cep3-1*, *cep3-2*, or *mif2-3* for *dam1-1* and *dam1-11*. However, *dam1-1* showed specific genetic interactions with *bir1*Δ and *ctf19*Δ. In total, these results suggest that the functions of Duo1p and Dam1p are closely interrelated and functionally linked to a specific subset of other proteins with diverse roles in mitotic spindle function.

Duo1p and Dam1p Are Required for Spindle Integrity

At the restrictive temperature, both *duo1* and *dam1* mutants arrested with a high percentage of large-budded cells (Fig. 2 A), suggesting a mitotic arrest. Double mutants between a *duo1* or *dam1* allele and a gene encoding a component of the spindle assembly checkpoint (*mad2*Δ or *mad3*Δ) did not arrest with large buds (Fig. 2 B), indicating that the large-budded arrest was dependent on the spindle assembly checkpoint.

Activation of the spindle assembly checkpoint by *duo1* and *dam1* mutants suggests that these mutants are sustaining spindle damage. Indeed, four classes of spindle defects were observed by immunofluorescence microscopy (Fig. 3). The first class of mutants (*duo1-2* and *dam1-9*; Fig. 3, A and C) arrested with a short spindle ~1–2 μm in length (see also Hofmann et al., 1998). However, when the spindle assembly checkpoint was eliminated, these mutants progressed through mitosis but showed slightly defective spindle structures, including bent and broken spindles (Fig. 3 B, arrow and Hofmann et al., 1998). The second class of mutants (*duo1*^{td} and *dam1-5*, not shown; *dam1-11*, and *dam1-1*, Fig. 3, G–J) showed a range of spindle defects including broken-down spindles (Fig. 3 G), elongated spindles with faintly staining microtubules in the middle of the spindle (Fig. 3 J), and spindles in which the spindle poles were separated but not connected by microtubules (Fig. 3, H and I). Some of

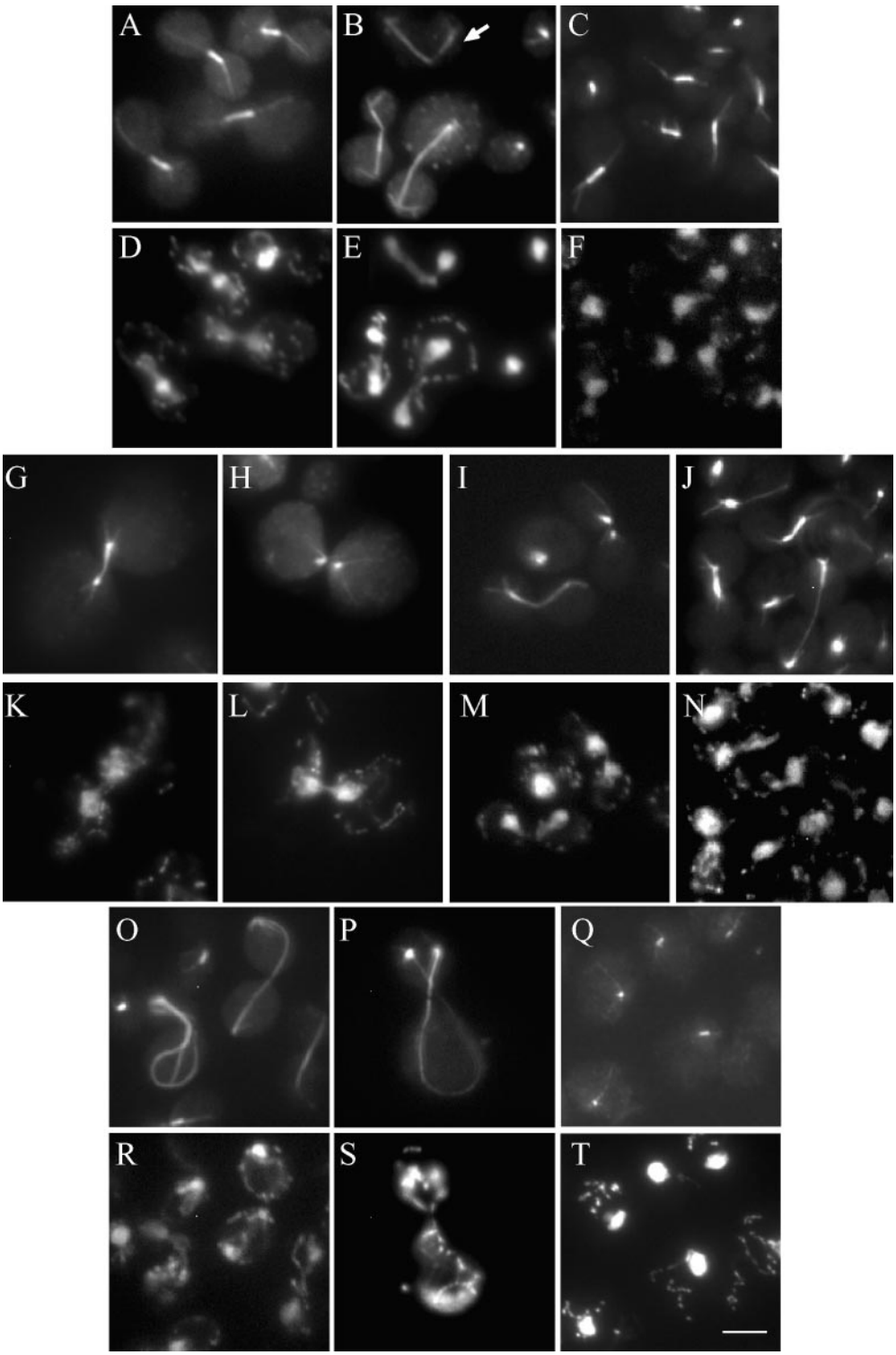

Figure 3. *duo1* and *dam1* mutants display diverse spindle defects. (A–C, G–J, and O–Q) Tubulin immunofluorescence of *duo1* and *dam1* mutants. (D–F, K–N, and R–T) The corresponding DNA (DAPI) staining. (A and D) *duo1-2*; (B and E) *duo1-2 mad2*Δ, arrow shows broken spindle; (C and F) *dam1-9*; (G, K and H, L) $duo1^{td}$; (I and M) *dam1-11*; (J and N) *dam1-1*; (O and R) *dam1-10*; (P and S) *duo1-1 dam1-1*; and (Q and T) *dam1-19*. Cells (A–N) were grown to log phase at 25°C, shifted to 37°C for 1.5 h. *dam1-10* is shown at 25°C. *duo1-1 dam1-1* is shown after 6 h at 37°C, though similar phenotypes are present at 25°C. *dam1-19* is shown after 4.5 h at 37°C. Bar, 5 μm.

these phenotypes are similar to those previously described for *dam1-1* (Jones et al., 1999). The third class (*dam1-10*; Fig. 3 O) showed ~5–10% hyperelongated spindles (≥10 μm), in addition to showing spindle phenotypes similar to the second mutant class. A similar phenotype was also observed for double mutants between *duo1-1* and *dam1-1* (Fig. 3 P). Although a slightly hyperelongated spindle phenotype has been described for mutations in *KIP3* (Straight et al., 1998), the hyperelongated spindles in the *dam1* mutants are much more dramatic and often wind around the cell. Colocalization with Tub4p, an SPB component, demonstrated that each end of these abnormal spindles contains an SPB (not shown). The final class of mutants (*dam1-19*; Fig. 3 Q) showed extremely short spindles (<1 μm). Even though these spindles were much shorter than a typical bipolar spindle, colocalization with Tub4p demonstrated that two separated SPBs were present in each spindle (not shown). A similar phenotype has also been observed for *slk19*Δ and *kar3*Δ mutants (Zeng et al., 1999), which show defects in stabilizing spindle microtubules.

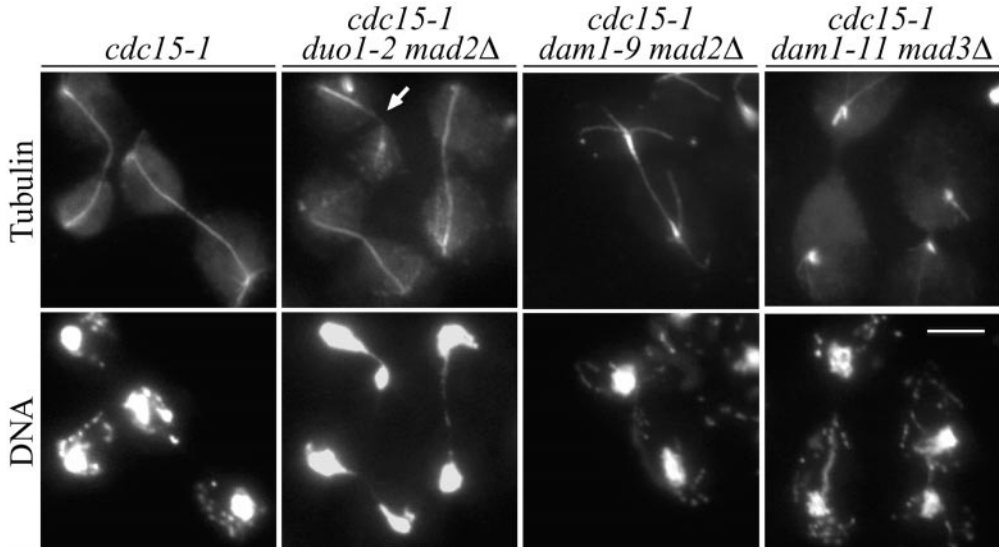

Figure 4. *duo1* and *dam1* mutants display distinct late mitotic phenotypes. Triple mutants between *duo1* or *dam1*, a spindle assembly checkpoint mutant (*mad2*Δ or *mad3*Δ), and a temperature-sensitive allele of *cdc15* were synchronized with alpha factor at 25°C and released into fresh prewarmed medium at 37°C. Samples were taken 2 and 3 h after alpha factor release and were processed for immunofluorescence and stained for tubulin (antitubulin antibody) and DNA (DAPI). Arrow shows *duo1-2* mutant spindle, which is broken. Bar, 5 μm.

Because *duo1* and *dam1* mutants show a checkpoint-dependent arrest, the phenotypes shown in Fig. 3 are representative of spindle morphology during metaphase. To test for spindle phenotypes at later time points in mitosis (Fig. 4), we eliminated the mitotic checkpoint (*mad2*Δ or *mad3*Δ) and blocked exit from mitosis using a *cdc15-1* mutant. *cdc15-1* ($Duo1^+Dam1^+$) cells arrested with an evenly stained, elongated mitotic spindle. Although *duo1-2* mutants showed relatively evenly stained spindle structures in late mitosis, some broken spindles were observed (Fig. 4, arrow). *dam1-9* mutants looked similar to *duo1-2* mutants during a metaphase arrest; however, *dam1-9* mutants arrested in late mitosis showed a broken-down spindle that stained faintly in the middle compared with wild-type spindles. *dam1-11* mutants showed an even more severe spindle breakdown phenotype in late mitosis in which the majority of cells had well-separated SPBs that were not connected by interpolar microtubules. The loss of interpolar microtubules in late mitosis has also been reported for *ase1*Δ mutants (Juang et al., 1997). These distinct phenotypes observed during both metaphase and late mitosis demonstrate important roles for Duo1p and Dam1p in different aspects of spindle integrity.

Electron Microscopy of duo1 and dam1 Mutants Reveals Splayed, Bent, and Broken Spindles

The budding yeast spindle has been characterized extensively by transmission electron microscopy of serial sections (Winey et al., 1995; O'Toole et al., 1997, 1999). Using this approach, we observed a range of ultrastructural defects in *duo1* and *dam1* mutants (Fig. 5). At the short spindle stage, *duo1-2* mutants showed a relatively normal bipolar spindle. However, compared with wild-type spindles in which the microtubules are packed closely together, *duo1-2* mutants showed some microtubules that splayed slightly outwards (Fig. 5 A, arrow), suggesting a defect in microtubule bundling. This lack of connection may underlie the bending or breaking of spindles in *duo1-2 mad2*Δ mutants (Fig. 5 B). We have observed this phenotype in multiple *duo1-2 mad2*Δ spindles. In some cases, elongated *duo1-2 mad2*Δ spindles were broken such that the half spindles made a 90° angle with each other. To further examine the spindles in mutants that have progressed past the short spindle stage, we examined the *dam1-9 mad2*Δ *cdc15-1* mutant discussed above (Fig. 5 C). Although the spindles in these mutants have elongated past 2 μm, there are still a large number of long microtubules that are very tightly bundled (Fig. 5 C, inset). In contrast, elongated spindles in wild-type cells show only a few microtubules which connect the two poles (Winey et al., 1995; O'Toole et al., 1999). In addition, some late mitotic *dam1-9* spindles were bent dramatically. By immunofluorescence, *dam1-10* mutants showed a variety of spindle defects even at the permissive temperature. Although electron microscopy of thin sections did not allow observation of the hyperelongated spindles, other spindle defects were observed. Many spindles showed one SPB that had invaginated into the nucleus (Fig. 5 D), suggesting a net decrease in outward spindle forces. In addition, as we also observed for other *duo1* and *dam1* mutants, the two halves of the bipolar spindle often failed to completely connect with each other. In such cases, although some microtubules ran between the SPBs (Fig. 5 D), a large number of microtubules extended beyond the opposite SPB (Fig. 5 E).

Duo1p and Dam1p Function Is Required during Mitosis

Although Duo1p and Dam1p contribute to spindle function, it is unclear when in the cell cycle their functions are required. The spindle assembly checkpoint is activated in *duo1* and *dam1* mutants, but a variety of defects can be sensed by this checkpoint. One possibility is that spindle damage is generated early in the cell cycle during spindle assembly. For example, *cdc31-2* and *mps2-1* mutants are defective in SPB duplication and arrest in mitosis due to the mitotic checkpoint (Weiss and Winey, 1996). A second possibility is that a defect, such as the inability to capture all of the kinetochores, occurs after the spindle has assembled. To determine when the activities of Duo1p and Dam1p are required for spindle function, *duo1* and *dam1* mutants were synchronized at 25°C with HU, which arrests cells in S phase with a short spindle structure. Mutants were released from this arrest to the restrictive temperature and scored for the percentage of large-budded cells. Wild-type and *duo1-2* mutant cells divided 60–80 min after

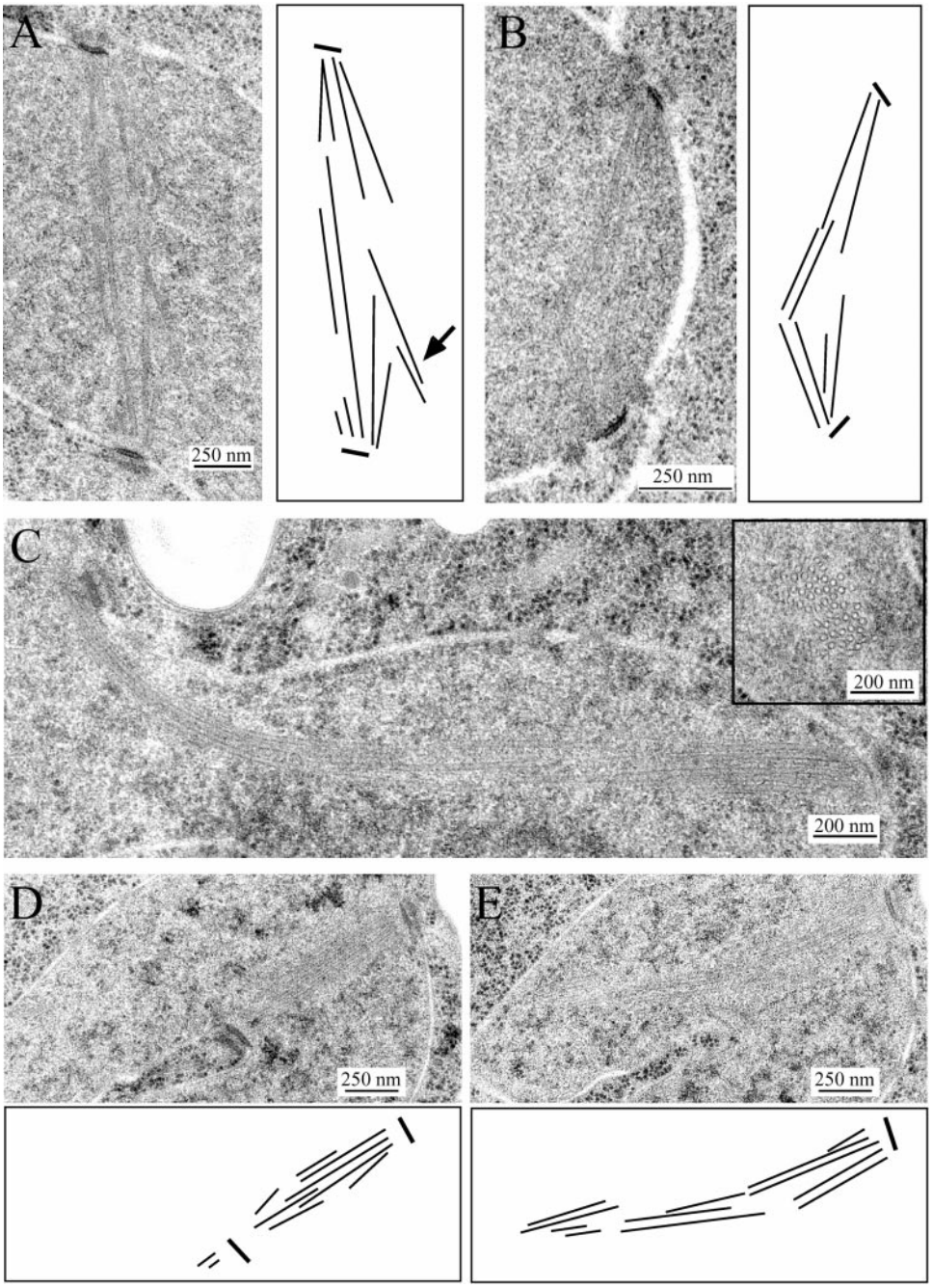

Figure 5. Electron microscopy of *duo1-2* and *duo1-2 mad2*Δ mutants. Thin sections (50 nm) of high pressure frozen yeast were viewed using transmission electron microscopy. (A) *duo1-2* mutant after 2 h at the restrictive temperature, showing a slightly splayed spindle and corresponding diagram showing positions of the microtubules. The arrow points to microtubules that splay outwards. (B) *duo1-2 mad2*Δ mutant after 2 h at the restrictive temperature, showing a slightly broken spindle and corresponding diagram showing positions of the microtubules. (C) *dam1-9 mad2*Δ *cdc15-1* mutant grown as in the legend to Fig. 4 showing a bent spindle. (C, inset) Cross section of this mutant showing a tight bundle of microtubules. (D and E) Two serial sections of *dam1-10* at the permissive temperature and corresponding diagrams showing one invaginated SPB and microtubules that fail to connect with the opposite pole.

HU release (Fig. 2 C). In contrast, *duo1*^{td} and most *dam1* mutants remained arrested at the large-budded stage, indicating a requirement for Duo1p and Dam1p function after spindle assembly has occurred. This arrest was also dependent on the spindle assembly checkpoint (Fig. 2 D).

To test the importance of Duo1p and Dam1p during spindle assembly, cells were first synchronized in G_1 using alpha factor and then allowed to form a spindle in HU at the restrictive temperature. Cells were then released into fresh medium lacking HU at the permissive temperature. Wild-type cells divided after ~120 min under these conditions. Although the majority of *duo1* and *dam1* mutants were able to divide when released to the permissive temperature, some mutants showed a delay in division compared with wild-type (Fig. 2 E). These results suggest either that these spindles are defective and must be repaired before the cells are able to progress through mitosis, or that after being lost at the restrictive temperature, Duo1p and Dam1p function is restored gradually after a shift back to the permissive temperature. To test more directly for the importance of Duo1p and Dam1p during spindle assembly, *duo1* and *dam1* mutants were synchronized in G_1 with alpha factor, then released to the restrictive temperature in the presence of 0.2 M HU. Treatment with HU, a DNA synthesis inhibitor, arrests yeast cells with large buds and short mitotic spindles. In contrast to the abnormal spindle phenotypes observed in the metaphase arrest (see Fig. 3, and below), *duo1-2*, *dam1-1*, *dam1-9*, *dam1-10*, *dam1-11*, and *dam1-19* all arrested with normal-looking short spindles, even after 4 h at the restrictive temperature (see Fig. 9 C). Similar results were also observed when 0.1 M HU was used (not shown). This result indicates that

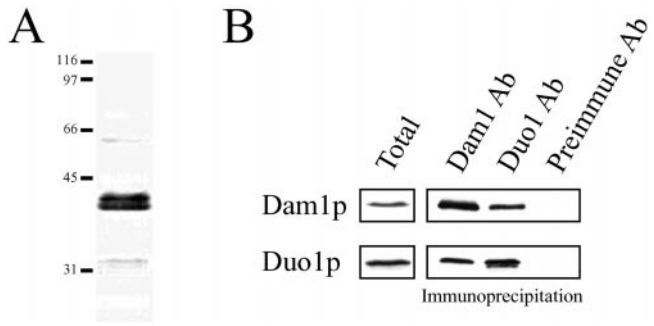

Figure 6. Dam1p and Duo1p physically associate in vivo. (A) Immunoblot of wild-type protein extract probed with anti-Dam1p antibodies. This antibody specifically recognizes bands between 39.5 and 42 kD, near the predicted size of 38.4 kD for Dam1p. (B) Duo1p and Dam1p coimmunoprecipitate out of yeast protein extracts. Yeast protein extracts were incubated with antibodies against Duo1p, Dam1p, or preimmune serum bound to protein A beads (see Materials and Methods). Immunoprecipitated samples were run on a 12% gel and probed with antibodies against either Dam1p or Duo1p. Duo1p and Dam1p are specifically immunoprecipitated when antibodies against either Duo1p or Dam1p are used but not with preimmune serum.

Duo1p and Dam1p function is not required to assemble a bipolar spindle, and that the function in spindle integrity is restricted to cells that have completed DNA synthesis.

Interdependence of Duo1p and Dam1p Function

Duo1p and Dam1p show a direct binding interaction in vitro and by two-hybrid analysis (Hofmann et al., 1998), suggesting that they might associate physically for their in vivo activity. To obtain evidence for this association, we generated an affinity-purified polycolonal antibody against Dam1p (see Materials and Methods). This antibody specifically recognized several protein bands 39.5–42 kD in immunoblots of yeast extracts (Fig. 6 A), near the predicted size of 38.4 kD for Dam1p. Using this antibody, Dam1p was immunoprecipitated from yeast protein extracts. As shown in Fig. 6 B, both Duo1p and Dam1p were immunoprecipitated with anti-Dam1p antibodies, indicating that these two proteins associate physically in protein extracts. Similarly, Duo1p and Dam1p are coimmunoprecipitated from yeast extracts when antibodies against Duo1p are used. In contrast, when guinea pig preimmune serum is used, neither protein is immunoprecipitated. In addition, tubulin is not immunoprecipitated by antibodies against either Duo1p or Dam1p (not shown).

We next determined whether Duo1p or Dam1p depend on each other for proper localization in vivo. *duo1* and *dam1* mutants were shifted to the restrictive temperature and stained with antibodies against Duo1p or Dam1p. As reported previously (Hofmann et al., 1998), Duo1p localizes to both the mitotic spindle and SPBs (Fig. 7 A). However, in both *duo1* and *dam1* mutants, Duo1p was delocalized. In the majority of *dam1* mutants, Duo1p was completely delocalized at the permissive temperature (not shown). In *dam1-9* (Fig. 7 C), staining is observed only at spindle poles at the permissive temperatures. At the restrictive temperature, Duo1p was completely delocalized. *duo1-2* mutants showed relatively normal Duo1p localization at the permissive temperature (not shown), but show only SPB localization after 3 h at 37°C (Fig. 7 C).

Similarly, Dam1p localized along the entire length of the mitotic spindle in wild-type cells (Fig. 7 B). These observations agree with previously reported localization of a GFP-Dam1p fusion protein expressed from the *GAL1* inducible promoter (Hofmann et al., 1998). In contrast, a Dam1-myc fusion protein expressed from the endogenous *DAM1* promoter localized primarily to spindle poles (Jones et al., 1999). The localization of Dam1p was disrupted in all *duo1* and *dam1* mutants at the permissive temperature (Fig. 7 D, *dam1-9* and *duo1-2*). These mutants showed a bright nuclear staining but did not show discernible spindle staining. Although *duo1* and *dam1* mutants show aberrant localization of Duo1p and Dam1p at the permissive temperature, the majority of these mutants do not show spindle or growth defects at this temperature. Duo1p and Dam1p are also completely delocalized when cells are treated with 20 μg/ml nocodazole for 2 h before immunofluorescence (Hofmann et al., 1998; and data not shown). Therefore, these experiments indicate that, in addition to microtubules, Duo1p and Dam1p require each other for their localization to the mitotic spindle. These effects are very specific since neither Duo1p or Dam1p appears delocalized in *mps1-1*, *cin8*Δ, *stu1-5*, *ase1*Δ, *bim1*Δ, *ndc10-2*, or *mad2*Δ mutants (not shown).

duo1 and dam1 Mutants Undergo Chromosome Missegregation at High Frequency

Previous studies suggested that lethality quickly occurs when *dam1-1* mutant cells are incubated at the restrictive temperature (Jones et al., 1999). To determine the reason for this lethality, we examined viability in several *duo1* and *dam1* mutants. As shown in Fig. 8 A, mutants that arrested with a short spindle (*duo1-2* and *dam1-9*) remained at least 50% viable after 4.5 h of incubation at 37°C. However, when the spindle assembly checkpoint was eliminated, viability decreased rapidly, with few cells remaining viable after 3 h at 37°C. The spindle assembly checkpoint was presumably able to prevent lethality of *duo1-2* and *dam1-9* mutants until later time points when these mutants break through their short spindle arrest. In contrast, other mutants (*dam1-1* and *dam1-11*) showed spindle elongation at the restrictive temperature despite the activity of the spindle assembly checkpoint (see Fig. 3). In these cases, it

Table IV. Frequency of Chromosome Missegregation in duo1 and dam1 Mutants

	Percent of cells with chromosome segregation defects		
	$t = 0$	$t = 1.5$	$t = 3$
	% (n)	% (n)	% (n)
Wild-type	0 (104)	1 (106)	0 (67)
dam1-1	3 (100)	99 (67)	81 (67)
dam1-11	0 (109)	88 (67)	84 (67)
*duo1-2 mad2*Δ	0 (47)	22 (67)	62 (50)

Cells were shifted to the restrictive temperature at $t = 0$ and chromosome missegregation was scored using LacI–GFP marked chromosomes. Only large-budded cells with a divided mass of DNA (as revealed by DAPI staining) were counted. A cell was scored as showing missegregation if two dots of LacI-GFP fluorescence were observed at the same pole, or if only one dot of LacI–GFP fluorescence was observed (corresponding to two chromatids that are too close to be resolved by light microscopy).

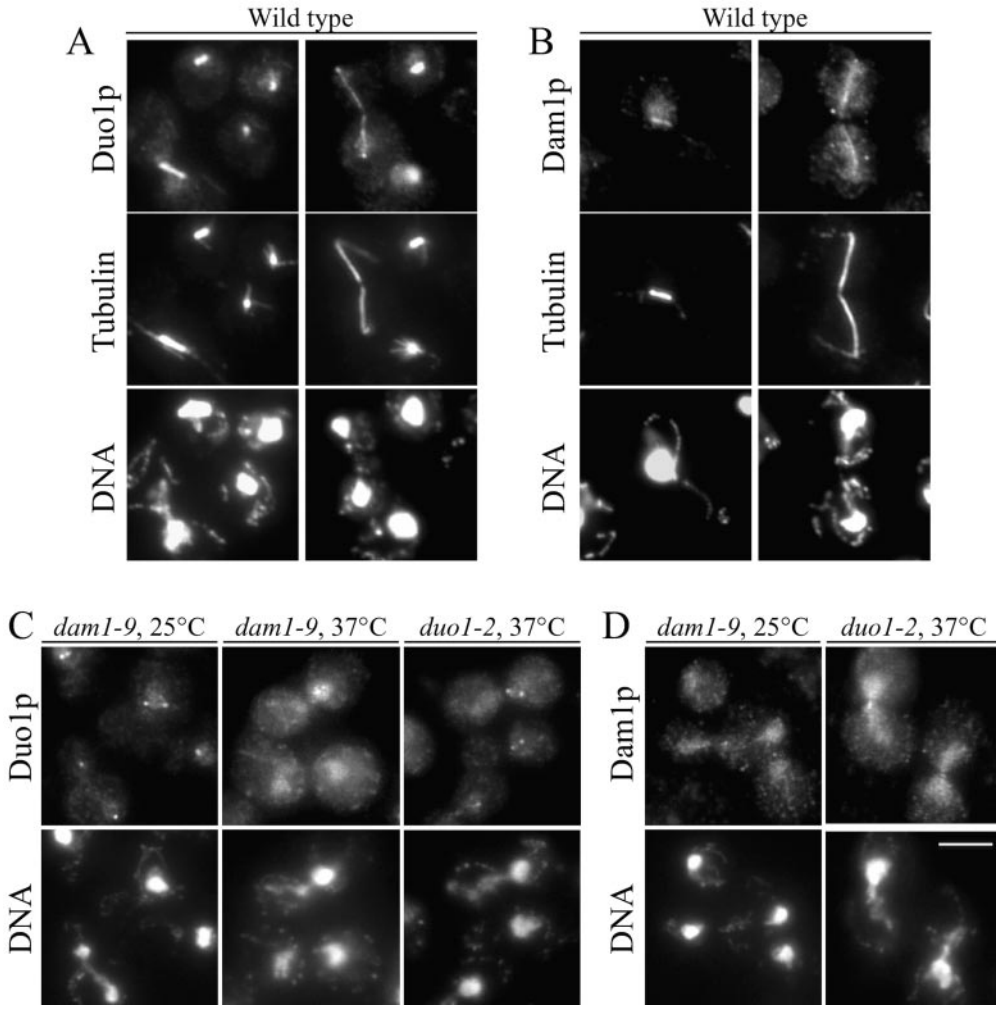

Figure 7. Duo1p and Dam1p show interdependent localization to the mitotic spindle. Wild-type, *duo1*, and *dam1* mutant cells were grown at 25°C, shifted to 37°C for 3 h, and then processed for immunofluorescence. (A) Wild-type cells stained for tubulin (antitubulin antibody), Duo1p (anti-Duo1p antibodies), and DNA (DAPI). (B) Wild-type cells stained for tubulin (antitubulin antibody), Dam1p (anti-Dam1p antibodies), and DNA (DAPI). (C) *duo1-2* and *dam1-9* mutants stained for Duo1p (anti-Duo1p antibodies) and DNA (DAPI). (D) *duo1-2* and *dam1-9* mutants stained for Dam1p (anti-Dam1p antibodies) and DNA (DAPI). Bar, 5 μm.

would be expected that the viability would drop more quickly. As shown in Fig. 8 B, *dam1-1* and *dam1-11* showed a dramatic drop in viability after only 3 h at 37°C. Eliminating the spindle assembly checkpoint in these mutants does have a small effect on viability at earlier time points, but overall the kinetics of cell death remain the same.

These results suggest that the decrease in viability observed in *duo1* and *dam1* mutants occurs as a result of spindle elongation and chromosome segregation. One possibility is that chromosome segregation is abnormal in these mutants, resulting in inviable aneuploid cells. To test this possibility, we monitored chromosome segregation by expressing LacI-GFP in a strain with 256 tandem copies of Lac operator sequence integrated on chromosome III (Straight et al., 1996). As shown in Fig. 8 C, *duo1* and *dam1* mutants missegregate chromosomes at the restrictive temperature. The frequencies of chromosome missegregation are reported in Table IV. Most notably, at 25°C, wild-type, *dam1-11*, and *duo1-2* mutant cells did not show any chromosome missegregation, whereas *dam1-1* showed only a very small frequency of missegregation. However, soon after any of these mutants was shifted to the restrictive temperature, the majority of cells showed chromosome missegregation. *dam1-1* and *dam1-11* mutants showed a level of chromosome missegregation that approached 100% in some cases, whereas *duo1-2* mutants showed a lower percent of missegregation.

Some dam1 Mutants Carry Out Anaphase-like Events While Arrested in Metaphase

dam1-1, dam1-5, *dam1-10*, *dam1-11*, and *duo1*^{td} mutants elongate their spindles and aberrantly segregate chromosomes despite the fact that these mutants activate the spindle assembly checkpoint (see Figs. 3 and 8 C). Because this checkpoint functions to inhibit the Cdc20p-bound form of the APC (Hwang et al., 1998), checkpoint activation should prevent degradation of the APC targets Pds1p and Clb2p (Cohen-Fix et al., 1996; Visintin et al., 1997) and arrest the cells in metaphase before sister chromatid separation and spindle elongation. Despite the fact that *duo1* and *dam1* mutants do not exhibit a spindle morphological arrest characteristic of metaphase, Pds1p and Clb2p are stabilized in these mutants at the restrictive temperature. After release from a permissive temperature HU block to 37°C, wild-type cells showed a 30-fold drop in Pds1p levels as they progressed through anaphase (Fig. 9 A). In contrast, *dam1-9* and *dam1-11* showed only a twofold decrease in Pds1p levels over the entire 150-min time course (Fig. 9 A). Immunofluorescence of these mutants showed that the vast majority of *dam1-9* and *dam1-11* nuclei stain for Pds1p even in cases where the DNA has separated (not shown). Similarly, although wild-type cells showed Clb2p degradation 60 min after release from HU, *dam1* mutants

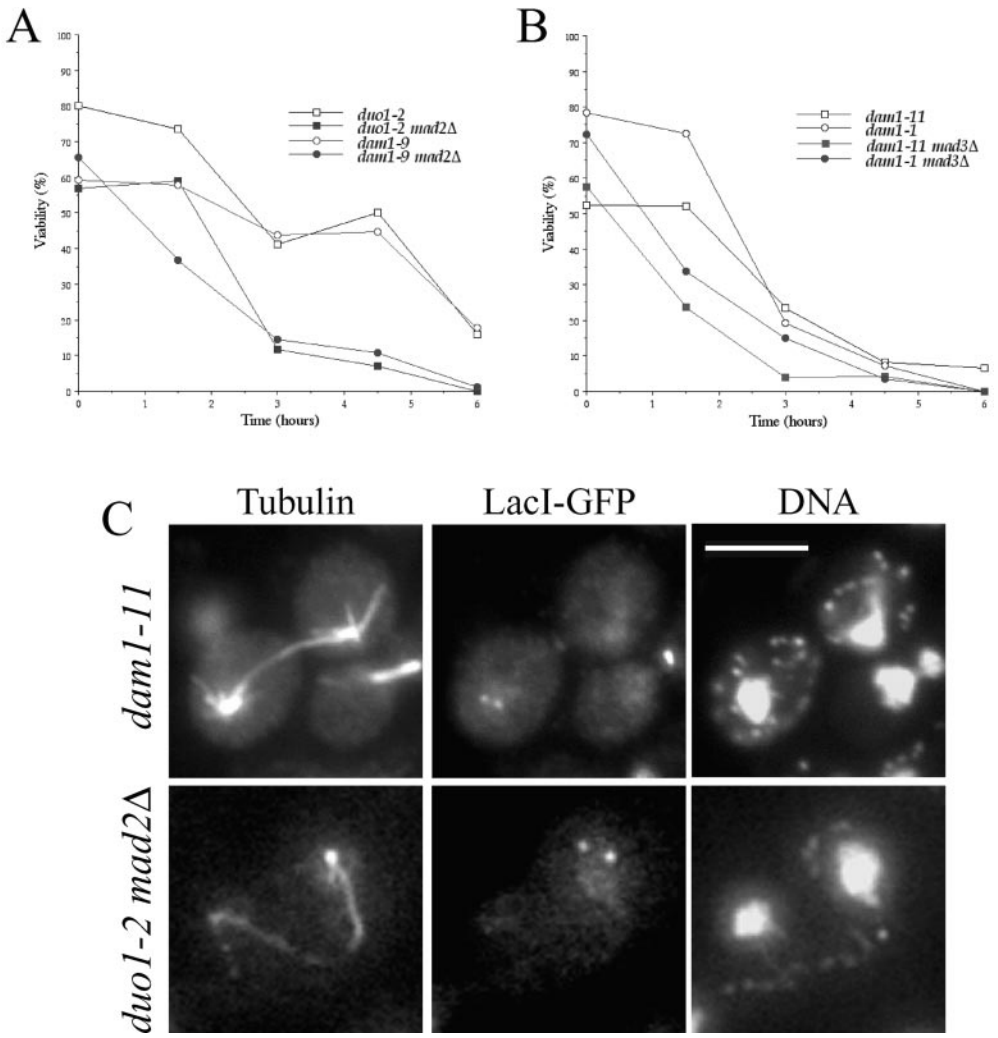

Figure 8. *duo1* and *dam1* mutants show chromosome missegregation. (A and B) Viability of *duo1* and *dam1* mutants. Cells were grown to log phase at 25°C, then shifted to 37°C at $t = 0$. For each time point, cells were plated onto YPD plates at 25°C, and a sample was counted in a hemacytometer to determine the cells per milliliter of culture. (A) Viability of mutants that arrest with a short mitotic spindle and of the corresponding double mutants with *mad2*Δ. (B) Viability of mutants that arrest with elongated spindles and of the corresponding double mutants with *mad3*Δ. (C) Chromosome missegregation is observed by LacI-GFP. Anti-GFP immunofluorescence of *duo1* and *dam1* mutants expressing LacI-GFP in a strain with multiple repeats of the LacO sequence integrated. Cells were synchronized with alpha factor, released into fresh medium at 37°C, and fixed for immunofluorescence after 3 h. Tubulin immunofluorescence, anti-GFP immunofluorescence to show the LacI-GFP fusion protein (each dot indicates a single chromatid), and DNA (DAPI) staining are shown for *dam1-11* and *duo1-2 mad2*Δ. The frequency of chromosome missegregation is tabulated in Table III. Bar, 5 μm.

actually showed a slight increase in Clb2p levels, demonstrating Clb2p stabilization (Fig. 9 B). These results indicate that the spindle assembly checkpoint inhibits the APC in *dam1* mutants.

It remained possible that some other aspect of APC function was not completely inhibited by the spindle assembly checkpoint in *duo1* and *dam1* mutants. Therefore, we sought to inhibit APC function directly through the use of temperature-sensitive mutations in subunits of the APC (*cdc16-1* or *cdc26*Δ) or a glucose-repressible *CDC20* that quickly arrests in metaphase in the presence of glucose. *cdc16-1* and *cdc26*Δ mutants arrest with virtually all cells having a large bud, a short metaphase length spindle, and a single mass of DNA (Fig. 9 D). Similar results were seen for double mutants between *cdc16-1* and *dam1-9,* which typically arrests with short spindles (not shown). However, in contrast to *dam1* mutants arrested in S phase with HU at the restrictive temperature (Fig. 9 C), double mutants between *cdc16-1* or *cdc26*Δ and *dam1-1*, *dam1-10*, or *dam1-11* had broken-down spindles, many with no microtubules connecting the SPBs (Fig. 9 D). Moreover, these spindles appeared to have elongated past the length of a normal metaphase short spindle, and two masses of DNA were segregated to the poles of these spindles. Thus, even when APC function was completely inhibited, some anaphase events, such as spindle elongation and chromosome segregation, occurred in a subset of *dam1* mutants. In contrast, if *dam1* mutants were allowed to form a metaphase spindle by arresting cells at the permissive temperature using a glucose-repressible *Gal-CDC20*, and were subsequently shifted to the restrictive temperature, no premature spindle elongation or chromosome segregation was observed (Fig. 9 E).

Premature anaphase events similar to those observed in the *dam1* APC^{ts} double mutants have been previously reported for double mutants between APC mutants and either cohesin mutants (Michaelis et al., 1997) or *ipl1* mutants (Biggins et al., 1999). In these cases, the authors suggested that spindle elongation occurred due to an inability to generate tension through the paired sister chromatids, either due to the absence of pairing or the inability of spindle microtubules to attach to both kinetochores. To

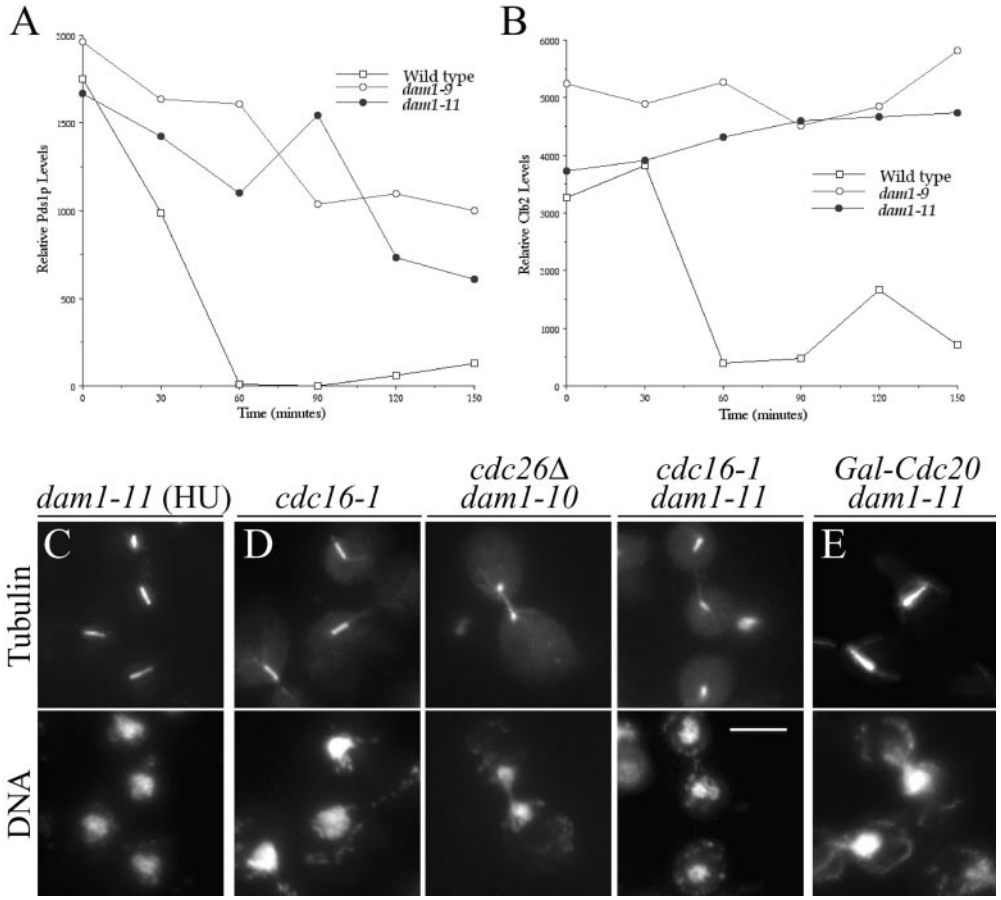

Figure 9. Some *dam1* mutants undergo anaphase-like events while under a metaphase arrest. (A and B) Pds1p and Clb2 levels after HU release. Cells were synchronized with alpha factor, released into medium containing 0.15 M HU but lacking alpha factor, and incubated for ~4.5 h at 25°C. The cells were then released into fresh prewarmed medium lacking HU at 37°C (t = 0). Protein samples were taken every 30 min and probed with anti-myc antibodies (9E10) against Pds1-myc18 or anti-Clb2 antibodies. Relative levels of Pds1p (A) or Clb2 (B) were quantified using a densitometer and were compared with β-tubulin levels as a loading control. (C) *duo1* and *dam1* mutants were synchronized with alpha factor at 25°C and released into fresh prewarmed medium at 37°C containing 0.2 M HU. They were then processed for immunofluorescence and stained with the YOL134 antibody against alpha tubulin. *dam1-11* is shown, but wild-type and other *duo1* and *dam1* mutants look identical. (D) Double mutants between *dam1* alleles and temperature-sensitive alleles of the APC (*cdc16-1* or *cdc26*Δ) were synchronized with alpha factor at 25°C and released into fresh prewarmed medium at 37°C. They were then processed for immunofluorescence as described above. (E) Double mutants between *dam1* and a galactose-inducible *CDC20* were grown in galactose and shifted to glucose for 2 h at 25°C to arrest the cells in metaphase. They were then shifted to 37°C for 2.5 h and processed as above. Bar, 5 μm.

test whether a cohesion defect was responsible for this effect in the *duo1* and *dam1* mutants, we examined sister chromatid separation in the presence of nocodazole, using the LacI-GFP system. In the absence of microtubules, sister chromatids remained paired (not shown), indicating that cohesion was not defective in these mutants.

Duo1p and Dam1p Localize to Kinetochores in Chromosome Spreads

Together with the high rate of chromosome missegregation, the premature anaphase events observed during a metaphase arrest suggested that kinetochore function might be defective in *duo1* and *dam1* mutants. To determine whether Duo1p and Dam1p are associated with kinetochores, we performed immunofluorescence on spreads of yeast chromosomes prepared as described (Loidl et al., 1998). This procedure removes the majority of the yeast cell, leaving the intact chromatin. Duo1p (Fig. 10 A) and Dam1p (Fig. 10 B) localized to punctate spots (usually one to four distinct loci) on the chromatin. Such a staining pattern is consistent localization to centromeric regions since it has been shown that centromeric regions are clustered in vivo (Jin et al., 1998). In addition, these punctate loci exactly colocalized with Ndc10p (Fig. 10, A and B), a well established kinetochore component (Goh and Kilmartin, 1993; Espelin et al., 1997; Meluh and Koshland, 1997). Identical results were also obtained using Mtw1-GFP (Goshima and Yanagida, 2000) as a marker for kinetochores (not shown). This localization was not dependent on microtubules, because antibodies against tubulin did not stain these chromosome spreads, and because Duo1p localized to chromosomes even when the cells were treated with 20 μg/ml nocodazole for 1 h before preparation of the chromosomes (not shown). Antibodies against the SPB component, Tub4p, do stain these chromatin spreads (Fig. 10, C and D). However, there are never more than one to two Tub4p foci per mass of DNA, consistent with the number of spindle poles associated with a nucleus. Although the Tub4p signal does overlap with some of the Ndc10p or Dam1p staining, there are multiple additional foci that do not colocalize with Tub4p (Fig. 10, C and D). In fact, some colocalization with kinetochores and SPBs is expected based on the clustering of centromeres around SPBs (Jin et al., 2000). These data suggest that, in addition to associating with intranuclear microtubules, Duo1p and Dam1p also associate with kinetochores. Duo1p and Dam1p are likely to be associated with kinetochores throughout the cell cycle because they

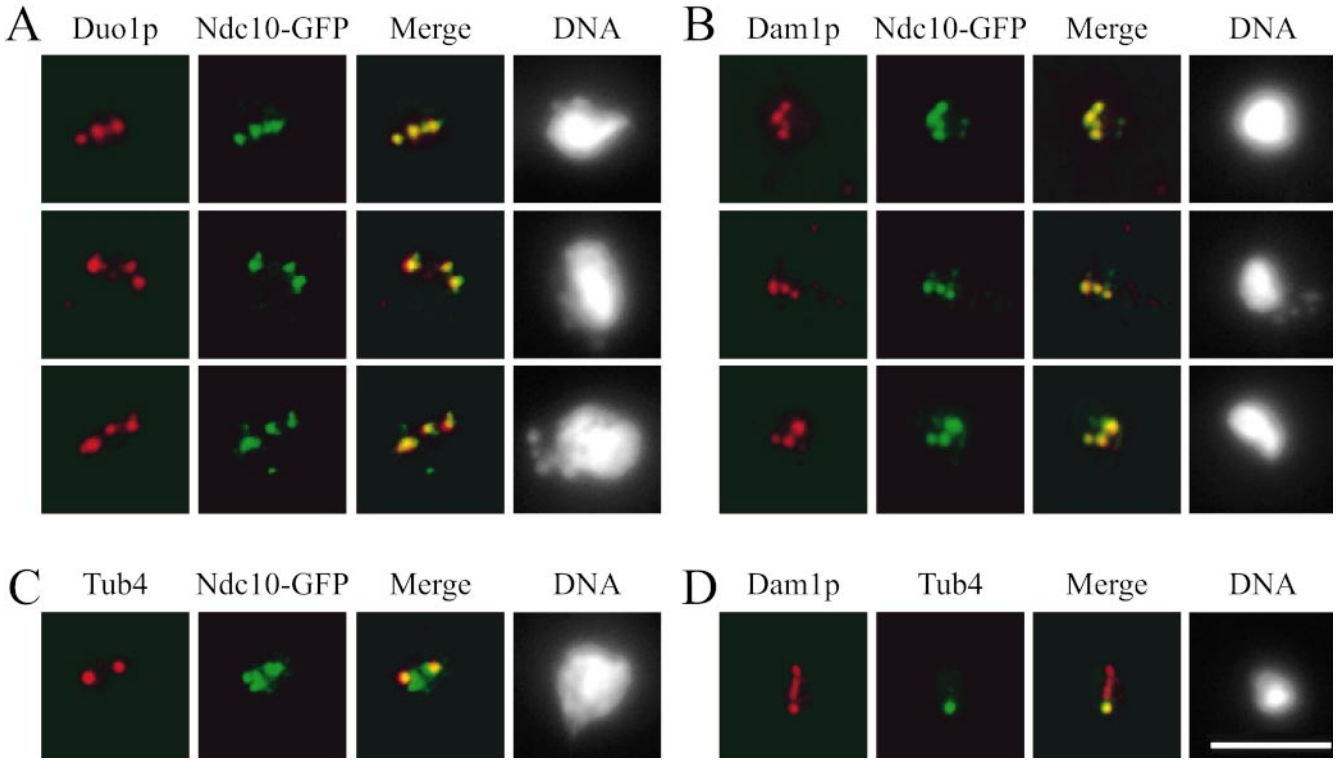

Figure 10. Duo1p and Dam1p localize to kinetochores. Cells expressing an Ndc10-GFP fusion protein were prepared for chromosome spreads as described (Loidl et al., 1998). They were then processed for immunofluorescence and stained with (A) anti-GFP antibodies to localize Ndc10-GFP (green) and antibodies against Duo1p (red), (B) anti-GFP (green) and anti-Dam1p (red) antibodies, (C) anti-GFP (green) and anti-Tub4p (red) antibodies, and (D) anti-Dam1p (red) and anti-Tub4p (green) antibodies. Bar, 5 μm.

were associated with every DNA mass in chromosome spreads prepared from logarithmically growing cells.

Discussion

Duo1p/Dam1p Form a Spindle-associated Protein Complex

Previous work demonstrated that Duo1p and Dam1p were able to associate physically (Hofmann et al., 1998). Here, we provide evidence that Duo1p and Dam1p functions as a complex in vivo. Duo1p and Dam1p coimmunoprecipitate from yeast protein extract and colocalize along the entire length of the mitotic spindle in a mutually dependent manner throughout the cell cycle. It would also be expected that mutations in any subunit of a complex would give rise to a similar range of phenotypes. We showed this to be the case for Duo1p and Dam1p with the short spindle arrest of *duo1-2* and *dam1-9* mutants, and with the similar range of abnormal spindle phenotypes associated with *dam1-1, dam1-5*, *dam1-11*, and *duo1*^{td}. In addition, genetic interactions between *duo1* and *dam1* alleles indicate that mutations in *DUO1* or in *DAM1* cause the cells to be specifically sensitive to mutations in the other gene, again supporting the conclusion that these proteins function as a complex.

Duo1p and Dam1p Function in Mitotic Spindle Integrity

Temperature-sensitive mutants of *duo1* and *dam1* display diverse defects that suggest a role in spindle integrity. Although some of these phenotypes have been observed individually in other yeast mutants, this striking range of very different phenotypes suggests that Duo1p and Dam1p may have multiple roles in maintaining spindle integrity. One possibility is that these defects reflect an inability to form cross-links between spindle microtubules. Such a role has been suggested for Ase1p, which localizes to the spindle midzone (Pellman et al., 1995). Dam1p has been shown to bind directly to microtubules (Hofmann et al., 1998), and it can interact with itself in the two-hybrid assay and in vitro (our unpublished results), suggesting that it can dimerize. Therefore, it is possible that the Duo1p/Dam1p complex binds to two separate spindle microtubules to provide spindle integrity. Although such an activity may explain some of the observed phenotypes, *ase1*Δ mutants do not show the dramatic hyperelongated spindles or very short spindles that we observed for *dam1* and *duo1* mutants. Therefore, the Duo1p/Dam1p complex appears to have additional spindle functions. Duo1p has recently been reported to interact physically with the microtubule-associated protein Bim1p in the two-hybrid system (Uetz et al., 2000). The allele-specific genetic interaction that we have identified between *dam1-1* and *bim1*Δ suggests that Bim1p may associate with the Duo1p/Dam1p complex for some aspect of spindle function.

Strikingly, the requirement for Duo1p and Dam1p function in spindle integrity appears to be restricted to cells that have completed DNA synthesis. Although the mitotic spindle assembles during S phase, additional changes must occur to the spindle before anaphase. During metaphase,

sister chromatids are subject to strong forces pulling towards the poles, such that anaphase initiation causes a fast separation of sister chromatids (Straight et al., 1997). Since sister chromatids are not present until DNA replication has been completed, these forces and the bipolar attachment of chromatids to the spindle must be established after spindle assembly. Although Duo1p and Dam1p are localized to the spindle throughout the cell cycle, SPB duplication and spindle assembly appear normal by immunofluorescence in *duo1* and *dam1* mutants. In fact, all of the *duo1* and *dam1* mutants were able to form normal-looking short spindles at the restrictive temperature when DNA replication was inhibited by HU. In contrast, abnormal spindle structures were observed when a subset of these mutants was arrested in metaphase using a temperature-sensitive APC mutant. These observations suggest that a change in spindle structure or forces occurs after DNA replication and that a requirement for Duo1p and Dam1p in the integrity of the mitotic spindle develops as a result of this transition.

A Role in Kinetochore Function

In addition to an important role for Duo1p and Dam1p in spindle integrity, we have also identified a novel role for this complex in kinetochore function. For all *duo1* and *dam1* alleles examined, a high level of chromosome missegregation occurred shortly after the shift to the restrictive temperature. One possibility is that the chromosome segregation defects are a result of the defects in spindle integrity. For example, a certain percentage of spindle microtubules might be destabilized in *duo1* or *dam1* mutants, leading to attachment of each pair of sister chromatids to a single spindle pole. However, due to the high frequency of missegregation and the fact that chromosome missegregation is observed regardless of the associated spindle phenotype, we favor an alternate model in which the Duo1p/Dam1p complex plays a more active role in chromosome segregation, possibly by serving as a link between the kinetochore and spindle microtubules. *dam1-1* and *dam1-11* mutants show 80–99% chromosome missegregation, a value that is consistent with mutants that affect kinetochore function: *ipl1* mutants show 70–85% missegregation (Biggins et al., 1999; Kim et al., 1999) and *ndc10-1* mutants show a complete failure to segregate chromosomes (Goh and Kilmartin, 1993).

A direct role in chromosome segregation is also suggested by the fact that some *dam1* mutants undergo spindle elongation and chromosome missegregation even when arrested in metaphase. Although it is possible that this effect is an indirect consequence of spindle integrity defects or abnormal spindle forces, other mutants that exhibit similar aberrant metaphase spindle elongation have been shown to affect kinetochore or cohesin function (Michaelis et al., 1997; Biggins et al., 1999). In these cases, since the spindle is unable to make bipolar attachments to paired sister chromatids, there is no tension to prevent the spindle from elongating. In fact, alleles of *dam1* that show spindle elongation during a metaphase arrest also show an extremely high frequency of chromosome missegregation. In contrast, *duo1* and *dam1* alleles that are able to arrest with a short spindle undergo a slightly lower frequency of chromosome missegregation, suggesting that enough bipolar attachments are correctly established to provide the tension required to maintain a short spindle.

Not only do *duo1* and *dam1* mutants have in vivo phenotypes indicative of a role in kinetochore function, but we have also found that Duo1p and Dam1p localize to kinetochores in spreads of mitotic chromosomes. Since Dam1p has been shown to bind directly to microtubules in vitro, these data raise the possibility that the Duo1p/Dam1p complex might serve as a structural or functional link between the kinetochore and the spindle microtubules. One possibility is that Duo1p and Dam1p play a role in establishing the connection between a new kinetochore and the mitotic spindle. Some *dam1* mutants show a frequency of chromosome missegregation that approaches 100%, and yet these mutants still show segregation of bulk DNA to each pole of the spindle. This suggests that one attachment to each pair of chromatids is functional. In contrast, *ndc10-1* mutants, which lack a functional kinetochore, show a complete failure to segregate chromosomes (Goh and Kilmartin, 1993). Some *dam1* mutants undergo premature chromosome segregation when arrested at metaphase at the restrictive temperature, suggesting a defect in attachments to the chromosomes (see above). In contrast, if these mutants are allowed to form a metaphase spindle at 25°C and are subsequently shifted to the restrictive temperature, no premature chromosome segregation occurs. This suggests that once bipolar attachments are made to each pair of sister chromatids, Dam1p function may no longer be required to maintain this attachment.

Although *duo1* and *dam1* mutants do not interact genetically with components of the CBF3 complex, we have observed genetic interactions with *bir1*Δ and *ctf19*Δ. Bir1p physically interacts with Ndc10p and also shows genetic interactions with mutants of other genes encoding kinetochore proteins (Yoon and Carbon, 1999). Ctf19p has been well established as a kinetochore protein (Hyland et al., 1999) and appears to act in a complex, together with Mcm21p and Okp1p, that may link to the CBF3 complex to other kinetochore proteins (Ortiz et al., 1999). In addition, we have observed genetic and physical interactions with *IPL1* (Cheeseman, I., J. Kang, and C. Chan, unpublished results), a protein kinase that regulates aspects of kinetochore function (Biggins et al., 1999). This last observation, in addition to observations by others showing that Dam1p interacts with Mps1p (Jones et al., 1999), a kinase with roles in SPB duplication and the mitotic checkpoint (Weiss and Winey, 1996), suggests that the activities that we have shown for the Duo1p/Dam1p complex in spindle integrity and kinetochore function may be regulated by protein phosphorylation during mitosis. Future studies will also address the mechanism by which Duo1p and Dam1p localize to kinetochores. One possibility is that these proteins associate with DNA directly through the putative leucine zipper domain of Dam1p (see Fig. 1).

The authors thank B. Goode, K. Kozminski, A. Rodal, C. Shang, J. Wong, E. Weiss, and S. Schuyler for discussions and advice. We also wish to thank Kent McDonald and the University of California at Berkeley Electron Microscope Laboratory for help and advice; Michele (Shelly) Jones and Mark Winey for sharing results, reagents, helpful discussions, and critical reading of the manuscript; Sue Biggins, Lena Hwang, and Andrew Murray for strains, advice, and helpful discussions; Doug Kellogg for the anti-Clb2 antibody, Pam Silver for the anti-GFP antibody; and Tim

Stearns for the anti-Tub4 antibody.

This work was supported by a grant from the National Institute of General Medical Sciences (GM-47842) to G. Barnes and a National Science Foundation Graduate Research fellowship to I.M. Cheeseman.

Submitted: 2 August 2000
Revised: 15 November 2000
Accepted: 17 November 2000

References

Ayscough, K.R., and D.G. Drubin. 1998. Immunofluorescence microscopy of yeast cells. *In* Cell Biology: A Laboratory Handbook. Vol. 2. J. Celis, editor. Academic Press, New York. 477–485.

Belmont, L.D., and D.G. Drubin. 1998. The yeast V159N actin mutant reveals roles for actin dynamics in vivo. *J. Cell Biol*. 142:1289–1299.

Biggins, S., F.F. Severin, N. Bhalla, I. Sassoon, A.A. Hyman, and A.W. Murray. 1999. The conserved protein kinase Ipl1 regulates microtubule binding to kinetochores in budding yeast. *Genes Dev*. 13:532–544.

Botstein, D., D. Amberg, J. Mulholland, T. Huffaker, A. Adams, D. Drubin, and T. Stearns. 1997. The yeast cytoskeleton. *In* The Molecular and Cellular Biology of the Yeast *Saccharomyces*. J.R. Pringle, J.R. Broach, and E.W. Jones, editors. Cold Spring Harbor Laboratory Press, Cold Spring Harbor, NY. 1–90.

Chen, R.-H., D.M. Brady, D. Smith, A.W. Murray, and K.G. Hardwick. 1999. The spindle checkpoint of budding yeast depends on a tight complex between the Mad1 and Mad2 proteins. *Mol. Biol. Cell*. 10:2607–2618.

Ciosk, R., W. Zachariae, C. Michaelis, A. Shevchenko, M. Mann, and K. Nasmyth. 1998. An ESP1/PDS1 complex regulates loss of sister chromatid cohesion at the metaphase to anaphase transition in yeast. *Cell*. 93:1067–1076.

Cohen-Fix, O., J.M. Peters, M.W. Kirschner, and D. Koshland. 1996. Anaphase initiation in *Saccharomyces cerevisiae* is controlled by the APC-dependent degradation of the anaphase inhibitor Pds1p. *Genes Dev*. 10:3081–3093.

Dohmen, R.J., P. Wu, and A. Varshavsky. 1994. Heat-inducible degron: a method for constructing temperature-sensitive mutants. *Science*. 263:1273–1276.

Espelin, C.W., K.B. Kaplan, and P.K. Sorger. 1997. Probing the architecture of a simple kinetochore using DNA–protein crosslinking. *J. Cell Biol*. 139: 1383–1396.

Goh, P.-Y., and J.V. Kilmartin. 1993. NDC10: a gene involved in chromosome segregation in *Saccharomyces cerevisiae*. *J. Cell Biol*. 121:503–512.

Goshima, G., and M. Yanagida. 2000. Establishing biorientation occurs with precocious separation of the sister kinetochores, but not the arms, in the early spindle of budding yeast. *Cell*. 100:619–633.

Hardwick, K.G., R. Li, C. Mistrot, R.H. Chen, P. Dann, A. Rudner, and A.W. Murray. 1999. Lesions in many different spindle components activate the spindle checkpoint in the budding yeast *Saccharomyces cerevisiae*. *Genetics*. 152:509–518.

Hardwick, K.G., R.C. Johnston, D.L. Smith, and A.W. Murray. 2000. MAD3 encodes a novel component of the spindle checkpoint which interacts with Bub3p, Cdc20p, and Mad2p. *J. Cell Biol*. 148:871–882.

Hofmann, C., I.M. Cheeseman, B.L. Goode, K.L. McDonald, G. Barnes, and D.G. Drubin. 1998. *Saccharomyces cerevisiae* Duo1p and Dam1p, novel proteins involved in mitotic spindle function. *J. Cell Biol*. 143:1029–1040.

Hoyt, M.A., L. Trotis, and B.T. Roberts. 1991. *S. cerevisiae* genes required for cell cycle arrest in response to loss of microtubule function. *Cell*. 66:507–517.

Hwang, L.H., L.F. Lau, D.L. Smith, C.A. Mistrot, K.G. Hardwick, E.S. Hwang, A. Amon, and A.W. Murray. 1998. Budding yeast Cdc20: a target of the spindle checkpoint. *Science*. 279:1041–1044.

Hyland, K.M., J. Kingsbury, D. Koshland, and P. Hieter. 1999. Ctf19p: a novel kinetochore protein in *Saccharomyces cerevisiae* and a potential link between the kinetochore and mitotic spindle. *J. Cell Biol*. 145:15–28.

Jin, Q., E. Trelles-Sticken, H. Scherthan, and J. Loidl. 1998. Yeast nuclei display prominent centromere clustering that is reduced in nondividing cells and in meiotic prophase. *J. Cell Biol*. 141:21–29.

Jin, Q.-W., J. Fuchs, and J. Loidl. 2000. Centromere clustering is a major determinant of yeast interphase nuclear organization. *J. Cell Sci*. 113:1903–1912.

Jones, M.H., J.B. Bachant, A.R. Castillo, T.H. Giddings, and M. Winey. 1999. Yeast Dam1p is required to maintain spindle integrity during mitosis and interacts with the Mps1p kinase. *Mol. Biol. Cell*. 10:2377–2391.

Juang, Y.L., J. Huang, J.M. Peters, M.E. McLaughlin, C.Y. Tai, and D. Pellman. 1997. APC-mediated proteolysis of Ase1 and the morphogenesis of the mitotic spindle. *Science*. 275:1311–1314.

Kim, J.H., J.S. Kang, and C.S. Chan. 1999. Sli15 associates with the ipl1 protein kinase to promote proper chromosome segregation in *Saccharomyces cerevisiae*. *J. Cell Biol*. 145:1381–1394.

King, R.W., J.M. Peters, S. Tugendreich, M. Rolfe, P. Hieter, and M.W. Kirschner. 1995. A 20S complex containing CDC27 and CDC16 catalyzes the mitosis-specific conjugation of ubiquitin to cyclin B. *Cell*. 81:279–288.

Korinek, W.S., M.J. Copeland, A. Chaudhuri, and J. Chant. 2000. Molecular linkage underlying microtubule orientation toward cortical sites in yeast. *Science*. 287:2257–2259.

Laemmli, U.K. 1970. Cleavage of structural proteins during the assembly of the head of bacteriophage T4. *Nature*. 227:680–685.

Lee, L., J.S. Tirnauer, J. Li, S.C. Schuyler, J.Y. Liu, and D. Pellman. 2000. Positioning of the mitotic spindle by a cortical-microtubule capture mechanism. *Science*. 287:2260–2262.

Li, R., and A.W. Murray. 1991. Feedback control of mitosis in budding yeast. *Cell*. 66:519–531.

Loidl, J., F. Klein, and J. Engebrecht. 1998. Genetic and morphological approaches for the analysis of meiotic chromosomes in yeast. *Methods Cell Biol*. 53:257–285.

Meluh, P.B., and D. Koshland. 1997. Budding yeast centromere composition and assembly as revealed by in vivo cross-linking. *Genes Dev*. 11:3401–3412.

Michaelis, C., R. Ciosk, and K. Nasmyth. 1997. Cohesins: chromosomal proteins that prevent premature separation of sister chromatids. *Cell*. 91:35–45.

O'Toole, E.T., D.N. Mastronarde, T.H. Giddings, Jr., M. Winey, D.J. Burke, and J.R. McIntosh. 1997. Three-dimensional analysis and ultrastructural design of mitotic spindles from the cdc20 mutant of *Saccharomyces cerevisiae*. *Mol. Biol. Cell*. 8:1–11.

O'Toole, E.T., M. Winey, and J.R. McIntosh. 1999. High-voltage electron tomography of spindle pole bodies and early mitotic spindles in the yeast *Saccharomyces cerevisiae*. *Mol. Biol. Cell*. 10:2017–2031.

Ortiz, J., O. Stemmann, S. Rank, and J. Lechner. 1999. A putative protein complex consisting of Ctf19, Mcm21, and Okp1 represents a missing link in the budding yeast kinetochore. *Genes Dev*. 13:1140–1155.

Pasqualone, D., and T.C. Huffaker. 1994. STU1, a suppressor of a beta-tubulin mutation, encodes a novel and essential component of the yeast mitotic spindle. *J. Cell Biol*. 127:1973–1984.

Pellman, D., M. Bagget, Y.H. Tu, G.R. Fink, and H. Tu. 1995. Two microtubule-associated proteins required for anaphase spindle movement in *Saccharomyces cerevisiae* [published erratum in *J. Cell Biol*. 131:561]. *J. Cell Biol*. 130:1373–1385.

Roof, D.M., P.B. Meluh, and M.D. Rose. 1992. Kinesin-related proteins required for assembly of the mitotic spindle. *J. Cell Biol*. 118:95–108.

Rose, M.D., F.M. Winston, and P. Hieter. 1990. Methods in Yeast Genetics: A Laboratory Course Manual. Cold Spring Harbor Laboratory Press, Cold Spring Harbor, NY. 198 pp.

Rothblatt, J., and R. Schekman. 1989. A hitchhiker's guide to analysis of the secretory pathway in yeast. *Methods Cell Biol*. 32:3–36.

Saunders, W., D. Hornack, V. Lengyel, and C. Deng. 1997. The *Saccharomyces cerevisiae* kinesin-related motor Kar3p acts at preanaphase spindle poles to limit the number and length of cytoplasmic microtubules. *J. Cell Biol*. 137: 417–431.

Saunders, W.S., and M.A. Hoyt. 1992. Kinesin-related proteins required for structural integrity of the mitotic spindle. *Cell*. 70:451–458.

Schwartz, K., K. Richards, and D. Botstein. 1997. BIM1 encodes a microtubule-binding protein in yeast. *Mol. Biol. Cell*. 8:2677–2691.

Sikorski, R.S., and P. Hieter. 1989. A system of shuttle vectors and yeast host strains designed for efficient manipulation of DNA in *Saccharomyces cerevisiae*. *Genetics*. 122:19–27.

Sobel, S.G. 1997. Mini review: mitosis and the spindle pole body in *Saccharomyces cerevisiae*. *J. Exp. Zool*. 277:120–138.

Sorger, P.K., F.F. Severin, and A.A. Hyman. 1994. Factors required for the binding of reassembled yeast kinetochores to microtubules in vitro. *J. Cell Biol*. 127:995–1008.

Straight, A.F., A.S. Belmont, C.C. Robinett, and A.W. Murray. 1996. GFP tagging of budding yeast chromosomes reveals that protein-protein interactions can mediate sister chromatid cohesion. *Curr. Biol.* 6:1599–1608.

Straight, A.F., W.F. Marshall, J.W. Sedat, and A.W. Murray. 1997. Mitosis in living budding yeast: anaphase A but no metaphase plate. *Science*. 277:574–578.

Straight, A.F., J.W. Sedat, and A.W. Murray. 1998. Time-lapse microscopy reveals unique roles for kinesins during anaphase in budding yeast. *J. Cell Biol.* 143:687–694.

Tirnauer, J.S., E. O'Toole, L. Berrueta, B.E. Bierer, and D. Pellman. 1999. Yeast Bim1p promotes the G1-specific dynamics of microtubules. *J. Cell Biol.*145:993–1007.

Uetz, P., L. Giot, G. Cagney, T.A. Mansfield, R.S. Judson, J.R. Knight, D. Lockshon, V. Narayan, M. Srinivasan, P. Pochart, et al. 2000. A comprehensive analysis of protein-protein interactions in *Saccharomyces cerevisiae*. *Nature*. 403:623–627.

Visintin, R., S. Prinz, and A. Amon. 1997. CDC20 and CDH1: a family of substrate-specific activators of APC-dependent proteolysis. *Science*. 278:460–463.

Weiss, E., and M. Winey. 1996. The *Saccharomyces cerevisiae* spindle pole body duplication gene MPS1 is part of a mitotic checkpoint. *J. Cell Biol.* 132:111–123.

Winey, M., C.L. Mamay, E.T. O'Toole, D.N. Mastronarde, T.H. Giddings, Jr., K.L. McDonald, and J.R. McIntosh. 1995. Three-dimensional ultrastructural analysis of the *Saccharomyces cerevisiae* mitotic spindle. *J. Cell Biol.* 129: 1601–1615.

Winsor, B., and E. Schiebel. 1997. Review: an overview of the *Saccharomyces cerevisiae* microtubule and microfilament cytoskeleton. *Yeast*. 13:399–434.

Yoon, H.J., and J. Carbon. 1999. Participation of Bir1p, a member of the inhibitor of apoptosis family, in yeast chromosome segregation events. *Proc. Natl. Acad. Sci. USA*. 96:13208–13213.

Zeng, X., J.A. Kahana, P.A. Silver, M.K. Morphew, J.R. McIntosh, I.T. Fitch, J. Carbon, and W.S. Saunders. 1999. Slk19p is a centromere protein that functions to stabilize mitotic spindles. *J. Cell Biol.* 146:415–425.